Applied Thermal Engineering 236 (2024) 121874

Contents lists available at ScienceDirect

Applied Thermal Engineering

journal homepage: www.elsevier.com/locate/apthermeng

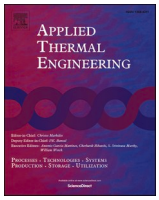

Research Paper

Improving thermal performance of groups of energy screw piles with phase change materials

Luis A. Bandeira Neto, Wenbin Fei *, Guillermo A. Narsilio

Department of Infrastructure Engineering, The University of Melbourne, Grattan Street, Parkville, VIC 3010, Australia

ARTICLE INFO

Keywords:
Geothermal engineering
Screw pile
Phase change material
Ground source heat pump
Numerical model

ABSTRACT

Underground thermal storage systems have potential to play an important part in the transition to renewable energy. Studies on combining building foundations with thermal storage are often limited to concrete piles, especially when involving phase change materials. In a recently published work, the authors presented a novel energy pile built using a screw pile filled with phase change materials. While the previous work considers all energy screw piles with same pile fillings, meaning a trade-off of low thermal conductivity and high heat capacity, screw piles in this work have two different functions: one screw pile filled with grout acts as the heat exchanger (energy pile) and its neighbour, filled with Phase Change Materials, act as a thermal battery (thermal storage pile). U-loop pipes are embedded only into the energy piles and connected to a Ground Source Heat Pump, so thermal energy from buildings will be stored in both the ground and the thermal storage piles. Numerical results show that this system can store up to 189.8 MJ/m^3 heat energy during one year of operation. The Coefficient of Performance of the heat pump increases slightly, up to 3.4 %, which results from an improvement of the cooling mode performance.

1. Introduction

Screw piles are an established foundation technology recognized for their cost-effectiveness and simple eco-friendly construction procedure. A screw pile consists of structural steel tubular elements, with one or more screw plates welded to its external wall, which is quickly inserted into the ground by a rotary hydraulic powerhead. This easy and fast construction procedure requires only light equipment, already reducing carbon footprint in comparison to bored piles [1–3]. This environmental benefit can be increased further if the screw piles are used to extract renewable shallow geothermal energy, by being converted into heat exchangers of a ground source heat pump (GSHP) system which are also known as energy screw piles [4–6]. The screw pile is one type of many energy structures that embed high-density polyethylene (HDPE) pipe circuits to perform heat exchange with the surrounding ground [7,8]. Energy structures were also used for seasonal thermal energy storage applications in which underground soil is the medium to store energy, but its capacity is limited [9]. Both geothermal energy extraction and seasonal thermal energy storage contribute to becoming carbon neutral by 2050 [10]. Therefore, improving the effectiveness of such systems is important.

Different from cast-in-place concrete piles, screw piles are hollow elements so that a backfill material is required to fill the space between the HDPE pipes and the pile wall to provide thermal contact (i.e., enhanced heat transfer from the pipe to the soil). Murari et al. [11] evaluated experimental tests in driven steel tubular piles filled with water, saturated sand and two different types of grouts, concluding that employing fillings with an increased thermal conductivity reduces thermal resistance and increases the heat exchange rate of the pile.

Phase Change Materials (PCM) are defined as materials that absorb and release substantial amounts of latent heat at a constant temperature during the phase change process (typically a solid–liquid transition) [12]. Hence, backfilling the pile with PCM is an option that could increase thermal storage capacity and rapid response of geothermal systems. The selection of the correct PCM requires the evaluation of several criteria, such as its thermal properties (e.g., latent heat, heat capacity, thermal conductivity), cost, corrosiveness, supercooling (i.e., the difference between melting and solidification temperatures) and toxicity [13]. PCMs can be classified into organic (paraffin and non-paraffin), inorganic (salt hydrates, metallic alloys and molten salts) and eutectic (mixtures of one or more PCM) [14]. Typically, inorganic PCMs have higher thermal conductivities than organic ones. However, inorganic PCMs present liabilities such as the high corrosivity of salt hydrates [15]

* Corresponding author.
E-mail address: wenbin.fei@unimelb.edu.au (W. Fei).

https://doi.org/10.1016/j.applthermaleng.2023.121874
Received 3 July 2023; Received in revised form 29 September 2023; Accepted 25 October 2023
Available online 29 October 2023

Nomenclature

CCOP	GSHP coefficient of performance for cooling operation only
COP	GSHP coefficient of performance
COP_{change}	Change in the GSHP coefficient of performance (from Reference to PCM case)
cp	Specific Heat Capacity, J/(kg•K)
D	Screw pile helix diameter, m
EP	Energy Screw Pile
GSHP	Ground Source Heat Pump
HCOP	GSHP coefficient of performance for heating operation only
HDPE	High-density polyethylene
L	Latent Heat, kJ/kg
P_s	Pile spacing, m
PCM	Phase Change Material
Q_{Ground}	Thermal load rejected/extracted from the ground
$Q_{Building,}$	Thermal load required by the building
q	circulating fluid flow rate, m^3/s
T	Temperature, °C
$T_{f,diff}$	Carrier fluid temperature difference (from Reference to PCM case), °C
T_{pc}	Phase change temperature, °C
TSP	Thermal Storage Pile
Θ	Phase state function of the PCM material
λ	Thermal conductivity, W/(m•K)
ρ	density, kg/m^3

Subscripts

f	Circulating fluid
g	Ground
in	Inlet circulating fluid temperature
out	Outlet circulating fluid temperature
PCM,l	Phase Change Material, liquid state
PCM	Phase Change Material
PCM,s	Phase Change Material, solid state
Ref	Reference case model

and high melting temperatures of metallic alloys [16]. PCMs can be used in the building industry in either active or passive applications, where in active applications the PCM phase change is activated/assisted by a powered device [17,18], such as a heat pump in a GSHP system.

There are a few studies regarding the employment of PCMs to improve borehole heat exchangers and GSHP systems performance. Chen et al. (2018) [19] evaluated the performance of a GSHP operating with a borehole filled with either grout, paraffin or inorganic salt hydrate PCM. The paraffin has a higher latent heat, while the inorganic PCM had a higher thermal conductivity, slightly lower than the grout. The authors concluded that the low thermal conductivity of the paraffin jeopardizes the GSHP performance to the point where its higher latent heat is not able to compensate. Meanwhile, the borehole with inorganic PCM provides a higher heat exchange rate than the grout, showing that incorporating latent heat storage into the borehole is beneficial to GSHP performance as long as the thermal conductivity is not reduced. Cortes et al. (2019) [20] evaluated the impact on the heat exchange rate caused by the latent heat of PCM introduced in a single borehole using numerical models, considering filling materials with different melting temperatures and comparing them to a non-PCM filling. The results showed that the PCM in the backfill increases heat exchange and reduces the thermal radius of the borehole, as the required design length by lowering the peak fluid temperature. These reductions were more noticeable when the phase change temperature (T_{pc}) value considered was the average between the peak fluid temperature and the undisturbed ground temperature. Aljabr et al. (2021) [21] compared the heat exchange performance of a borehole filled with grout and another with organic PCM that has lower thermal conductivity. Similar to Cortes et al. (2019) [20], the conclusion presented was that the T_{pc} should be chosen accordingly to the peak fluid temperature and undisturbed ground temperature. In addition, the results showed that the borehole design length can be reduced by adding PCM in the borehole backfill. However, the GSHP performance is jeopardized by the lower thermal conductivity of the PCM. The disadvantages of the low thermal conductivity of PCM to the heat transfer of underground heat exchangers are present in another handful of studies [22,23].

Studies on the utilisation of energy piles and PCM are less common. Yang et al. (2021) [24] used a scale laboratory test (24 h duration) to conclude that incorporating encapsulated paraffin PCM in a concrete energy pile increases heat exchange and can reduce pile deformation by keeping the temperature stable. Mousa et al. (2020) [25] also tested a reduced scale model of an energy pile in the laboratory, but implementing PCM-filled cylindric containers in piles rather than directly mixing with concrete. The results show an increased heat exchange rate within the pile with PCM in comparison to the reference model (only concrete, no PCM), but the test is even shorter (3 h). In the following work from the same authors, the experiment is used to validate a finite element (FE) model, used to perform a long-term analysis of a single large pile (1.5-metre diameter) attending a real hourly thermal load [26] for a whole year. The results showed that the GSHP system benefits the most from the PCM in the pile when the phase change process is underway. When the latent heat available was depleted, the lower thermal conductivity of the PCM reduced the performance in comparison to the pure concrete pile. Nevertheless, the overall impact of PCM in the referred study case is positive. Alavy et al. (2021) [27] simulated a similar large diameter pile (1.4 m) with PCM cylinders for one year under operation. The conclusions were also in favour of PCM usage, which improved performance in comparison to traditional vertical ground heat exchangers. However, incorporating PCM in the concrete can reduce its compression resistance significantly [28,29]. Special types of cement that incorporate composite PCM such as the graphite nanoplatelet-based PCM (GNP-Paraffin) presented by Bao et al. (2017) [30] are an alternative that could avoid the loss of structural performance. While these studies covered concrete piles, no work on PCM energy screw piles could be found besides our recently published paper [31]. In that work, several PCM mixtures were tested as backfill of a single energy screw pile, showing that the mixtures with a higher latent heat provide increased heat exchange and reduced thermal radius. Still, the heat exchange is more sensitive to the thermal conductivity of the backfilling than to the latent heat. In summary, work to date shows that the latent heat transferred from/to the PCM enhances the heat exchange rate during the phase change process, but the thermal conductivity is more important for the heat transfer in the long run.

However, the aforementioned studies considered only energy pile elements with the same function. Within the few studies on energy piles, only a limited work performed long-term analysis (e.g., one year) which captures both periods with and without PCM phase transition. In the present work, a numerical model was validated and used to analyse the performance of a novel underground heat exchanger system based on energy screw piles. Since screw piles tend to be short when used as building foundations, a lot of them are required to provide structural support. In the new system, part of these piles are used as heat exchangers (energy screw piles as in Bandeira Neto et al. (2023) [4], shown later in Fig. 3a as "EP"), while the remaining/adjacent screw piles have the steel shell filled with PCM (shown later in Fig. 3a as "TSP"), exchanging (and storing) heat energy passively due to the temperature

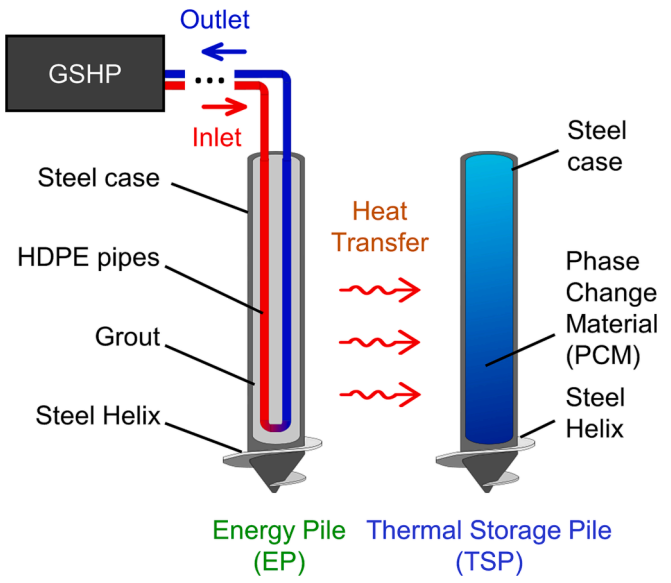

Fig. 1. Graphical description of the proposed underground heat exchanger system involving Energy Piles (EP) and Thermal Storage Piles (TSP).

variation induced by energy screw piles. In this system, the PCM is not in direct contact with the pipes as it happens in the other existing studies, which is expected to reduce the negative effects of its low thermal conductivity on the heat exchange.

2. Methodology

This section presents the rational for the proposed underground heat exchanger system and the numerical model used to perform the analyses. A phase change feature was implemented into a model built in COMSOL Multiphysics [32], previously validated against a field-scale thermal response test executed on an energy screw pile [4]. For the validation of the phase change modelling, a geometry based on a laboratory test executed on a scaled model of a concrete energy pile was built [25].

2.1. Proposed underground heat exchanger system

The underground heat exchanger system proposed in this work considers energy screw piles as the primary underground heat exchangers while the remaining screw piles filled with PCM are used as thermal storage piles. Since screw piles have small diameters, a large number of them is required to form a strong foundation for buildings. Then, if using all piles as energy piles by installing HDPE pipes in each of them, the narrow spacing will lead to severe thermal interference since the thermal radius around the pile is larger than the pile spacing. As a result, the energy pile system may render a low performance [4,33,34]. Since not every screw pile is preferred to be an energy screw pile (EP), this work proposes to use these redundant piles as thermal storage piles (TSP) instead by filling them with Phase Change Material. As shown in Fig. 1, the EP is connected to the heat pump to exchange heat with the soil, while the TSP absorbs or rejects the heat energy according to the building's thermal energy demand. This approach also solves a challenge in the previous system that fills the EP with PCM since the low thermal conductivity of PCM hinders the heat exchange rate between the HDPE pipes and the soil around the EP.

2.2. Governing equations

The foundation of the model employed in this work couples heat transfer and fluid flow equations and has been presented in several published studies on energy structures [35–37]. The model considers both heat conduction and convection for the circulating fluid in HDPE pipes using (Eq. (1) and (2)), while only conduction is considered within the other materials (Eq. (3)). No groundwater is considered in the soil and so no convection heat transfer is considered neither in the soil nor the PCM, which is a conservative approach as these would increase the heat transfer [38,39]. The fluid flow model is based on both continuity and momentum equilibrium equations (Eq. (4) and (5), respectively). The pipes are modelled as one-dimensional elements, so the fluid temperature at a determined point in the pipe is the average temperature across its cross-sectional area. More on this model and several validation cases can be found in [32,40–43].

$$\rho_f A c_{p,f}\frac{\partial T_f}{\partial t}+\rho_f A c_{p,f} v \bullet \nabla T_f = \nabla \bullet \left(A\lambda_f \nabla T_f\right)+f_D\frac{\rho_f}{2d_h}|\boldsymbol{v}|\boldsymbol{v}^2+Q_{wall} \tag{1}$$

$$Q_{wall} = f\left(T_{pipewall}, T_f, \lambda_p, d_p\right) \tag{2}$$

$$\rho_m c_{p,m}\frac{\partial T_m}{\partial t} = \nabla \bullet \left(\lambda_m \nabla T_m\right) \tag{3}$$

$$A\rho_f \nabla \bullet \boldsymbol{v} = 0 \tag{4}$$

$$\rho_f\left(\frac{\partial \boldsymbol{v}}{\partial t}\right) = -\nabla p - f_D\frac{\rho_f}{2d_h}\boldsymbol{v}|\boldsymbol{v}| \tag{5}$$

where ρ_f is the circulating fluid density, A is the inner cross-section area of the HDPE pipes, $c_{p,f}$ is the fluid-specific heat capacity, T_f is the fluid temperature, t is the time, $\boldsymbol{v}$ is the fluid velocity vector field and λ_f is the fluid thermal conductivity. Q_{wall} stands for the external heat exchange rate through the pipe wall and is a function of the temperature on the pipe outer wall ($T_{pipe\ wall}$), the pipe wall thermal conductivity λ_p, the pipe diameter d_p and the fluid temperature. The solid heat conduction is governed by the material density ρ_m, the material specific heat capacity $c_{p,m}$, the material temperature field T_m and the material thermal conductivity λ_m. p is the pressure inside the pipes, f_D represents the Darcy friction factor and d_h is the hydraulic diameter of the pipes.

The phase change feature is introduced to the model using the equivalent specific heat capacity approach [26,31,32,44]. Eq. (3) is updated with the PCM material density (ρ_{PCM}), specific heat capacity ($c_{p,PCM}$) and thermal conductivity (λ_{PCM}), which vary according to its liquid/solid state. The $c_{p,PCM}$ and λ_{PCM} are determined by the phase composition of the PCM – liquid ($\theta_{PCM,l}$) or solid ($\theta_{PCM,s}$) (Eq. (7), (8), (9), and (10)). To keep mass conservation and exempt the model from considering the PCM volume change, the ρ_{PCM} value is deemed constant as an average between solid ($\rho_{PCM,s}$) and liquid ($\rho_{PCM,l}$) phase values. Experience with the models shows that the sensitivity to the materials' density on the heat transfer is significantly lower in comparison to the respective thermal conductivity and the latent heat.

$$\rho_{PCM} c_{p,PCM}\frac{\partial T_{PCM}}{\partial t} = \nabla \bullet \left(\lambda_{PCM}\nabla T_{PCM}\right) \tag{6}$$

$$c_{p,PCM} = \left(\theta_s c_{p,PCM,s}+\theta_l c_{p,PCM,l}\right)+L\frac{\partial m_i}{\partial T_{PCM}} \tag{7}$$

$$m_i = \frac{1}{2}\frac{\theta_{PCM,l}-\theta_{PCM,s}}{\theta_{PCM,s}+\theta_{PCM,l}} \tag{8}$$

$$\lambda_{PCM} = \theta_{PCM,s}\lambda_{PCM,s}+\theta_{PCM,l}\lambda_{PCM,l} \tag{9}$$

$$\theta_s+\theta_l = 1 \tag{10}$$

$$\rho_{PCM} = \frac{\rho_s+\rho_l}{2} \tag{11}$$

where L is the latent heat of fusion and m_i is the mass fraction function. The values of $\theta_{PCM,l}$ and $\theta_{PCM,s}$ are determined by a smooth function of the PCM temperature T_{PCM}, which varies from 0 to 1, to

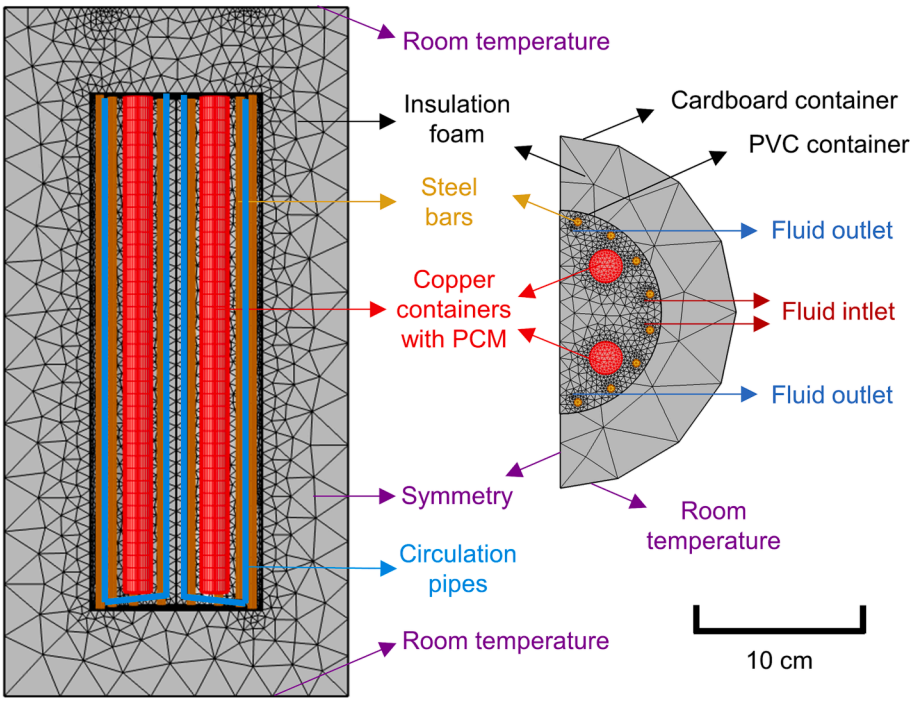

Fig. 2. Validation model of a phase change experiment: Geometry, materials and boundary conditions.

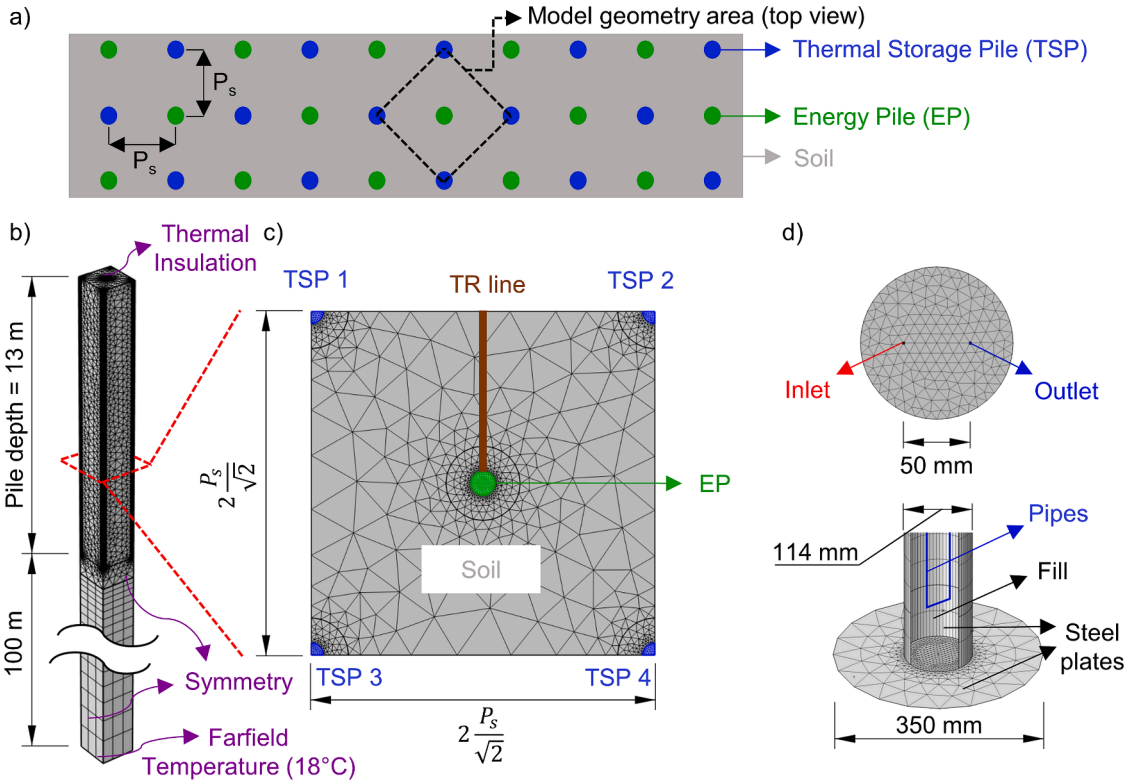

Fig. 3. Pile grid – evenly distributed with pile spacing P_s (a) and numerical model – full model with geometry mesh, boundary conditions (b) model top view (c) and energy screw pile cross-section and screw pile detail (d).

avoid sharp transitions and ensure model convergence. This function ensures the phase change process occurs smoothly within an interval around the value of T_{pc}. This interval is considered to be 4 °C, based on the selected PCM properties. Eq. (7) considers the latent heat effect by increasing the specific heat capacity of the material during the phase change process [32].

2.3. Validation

The laboratory test executed by Mousa et al. (2020) [25] was used to

Table 1
Material properties used for model analyses.

Material	Density ρ (kg/m^3)	Thermal conductivity λ (W/m·K)	Specific heat capacity c_p (J/kg K)	Latent heat L (kJ/kg)
Ground* [4]	2000	1.5	830	–
Grout [4]	2250	1.6	890	–
Steel [32]	7850	44.5	475	–
Air [32]	1.225	0.025	1005	–
PCM (liquid) [47]	750	0.18	2400	206
PCM (solid) [47]	789	0.19	1800	

* The effects of the ground thermal conductivity are evaluated in this work. See Table 2.

validate the model that includes PCM, apart from the validation previously undertaken for a field scale energy pile group [4]. The experimental setup consists of a scaled concrete pile with four PCM cylindric containers and four copper pipe U-loops embedded in the concrete (Fig. 2). The pile is covered by a thick layer of insulation foam, and the water at a constant temperature is circulated in the pile through copper pipes to provoke a phase change process on the material inside the containers. Considering the inlet fluid temperature recorded during the test as an input of the numerical model, the calculated outlet fluid temperature and the temperature mid-depth in the PCM cylinder are compared with corresponding experimental measurements for validation. All other details on the experiment, the material parameters and the test results used in this model validation can be found in Mousa et al. [25]. The model geometry built for the test simulation and its boundary conditions are presented in Fig. 2.

2.4. Numerical model

With the model validated, a new geometry was built to analyse the performance of the proposed underground heat exchanger system presented in Section 2.1. Using the individual energy screw pile geometry originally tested by Bandeira Neto et al. (2023) [4], the model considers a group of piles distributed in a grid (Fig. 3a) using symmetry boundaries. Only half of the piles in the grid are thermally activated (i.e., exchange heat actively), with a single HDPE 32 mm (outer diameter) pipe U-loop installed inside the steel case of the hollow screw pile before being filled with grout (green piles in Fig. 3). The remaining screw piles (hereafter thermal storage piles (TSP), marked in blue in Fig. 3) exchange and store heat passively, considering the filling as air (i.e., empty) or PCM material. Fig. 3b), c) and d) presents increasing level of details of the geometry of the analysis model. A line is defined at mid-depth in the geometry, perpendicular to the model side boundary (TR line), to investigate the thermal radius. All the material properties (Table 1) result from the field test conducted in Melbourne [4] and the COMSOL materials library [32], except for the parameters of the PCM. The properties of the PCM are based on the organic PCM-RT material manufactured by Rubitherm [45]. The PCM-RT was considered in other studies that involve energy piles [27] and other thermal storage applications [46,47]. It has low corrosivity and low volume change [48]; these characteristics are important to avoid negative effects on the structural performance of the piles (e.g., steel case corrosion). The manufacturer states that the material is available in different formats (e.g., compact storage, microencapsulation) and in a wide range of phase change temperatures. The parameters of the PCM-RT material are selected referring to [47] while the phase change temperature varies along the conducted analyses. The model considers the initial undisturbed ground temperature as 18 °C typical of a temperate climate [49], defined as the constant temperature at the bottom boundary. The circulating fluid flow rate adopted is 5 L/min, enough to ensure turbulent flow conditions [50].

The model simulates the operation of the screw piles acting as energy structures of a GSHP system, considering the design thermal load of a large educational building located in Melbourne – Australia with a cooling/heating demand ratio of 1.8 (i.e., cooling dominant load, presented in Fig. 4). To keep the fluid temperatures within the heat pump's

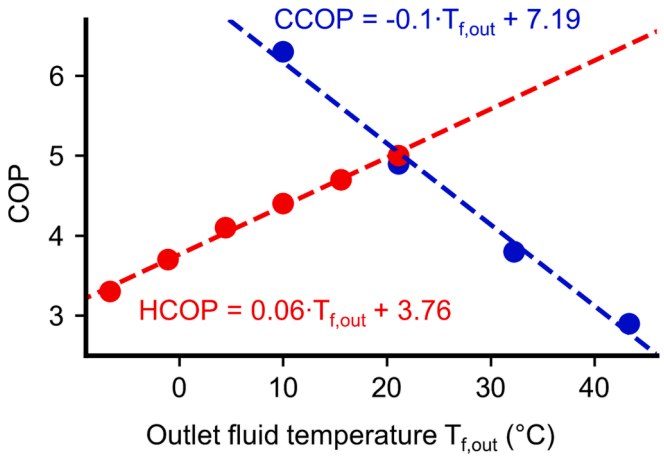

Fig. 5. Heating and Cooling COP values (HCOP and CCOP respectively) of the heat pump (CLIMATEMASTER TMW340 60 Hz I-P [51]).

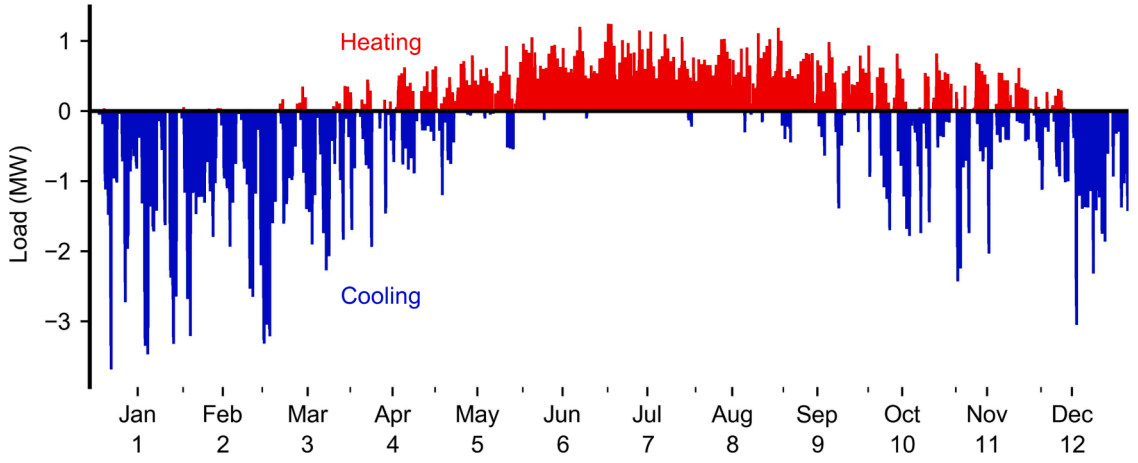

Fig. 4. Hourly thermal load of a building located in Melbourne – Australia considered in the simulations (winter in July) (Design data, October 28, 2020).

Table 2
Parameters considered in the parametric analysis.

Parameter	Values
Pile spacing (P_s)	2•D and 3•D (0.70 m and 1.05 m)
Ground thermal conductivity (λ_g)	1.5 W/(m•K) and 3.0 W/(m•K)
T_{pc} combination	Single and Mixed
Operational scheme	Full load and Cooling only

operational range, the load was scaled down by a factor of 7000. In other words, these many energy screw piles would be needed to satisfy 100 % of the thermal load, in practice the energy foundation solutions would satisfy the based load, a portion of this total as a lower count of pile is likely needed for the building foundation.

Using an hourly time step, the model is used to simulate a whole year of operation to capture both short-term and seasonal heat transfer characteristics. In this study, the model considers the Coefficient of Performance (COP) of the heat pump as recommended by Chen et al. (2018) [18], which depends on the fluid temperature entering the pump and the operation mode (heating or cooling). Fig. 5 presents the COP curves for the heat pump adopted in this study (CLIMATEMASTER TMW340 60 Hz I-P [51]). At each simulation time step (i.e., an hour), the load signal determines if the operation is either heating or cooling (positive and negative values, respectively), defining the use of either the heating COP (HCOP) or Cooling COP (CCOP) curves. Next, the fluid temperature coming out of the energy pile (therefore, into the heat pump) defines the COP value. The heat load being either extracted or rejected into the ground is determined from Eq. (12) and (13), and the inlet fluid temperature from Eq. (14).

$$Q_{Ground} = Q_{Building}\left(1 - \frac{1}{HCOP}\right) \tag{12}$$

$$Q_{Ground} = Q_{Building}\left(1 + \frac{1}{CCOP}\right) \tag{13}$$

$$T_{f,in} = T_{f,out} + \frac{Q_{ground}}{q \bullet \rho_f \bullet c_{p,f}} \tag{14}$$

where Q_{ground} is the thermal load rejected or extracted from the ground, $Q_{Building}$ is the thermal load required by the building, T_{in} and T_{out} are respectively the circulating water temperature going in and out of the energy screw pile and q is the circulating fluid flow rate. The electric energy consumed by the heat pump is the absolute difference between Q_{ground} and $Q_{Building}$.

2.5. Grid independency analysis

Due to the high computational costs involved in running this model resulting from combining an extensive simulation time (1 year) and small time-stepping (every hour) to capture both short and long-term effects, the mesh grid had to be optimised to ensure the results were grid independent while the time duration of the simulations was reasonable. The meshes for the piles are refined to ensure high precision (Fig. 3) while the number of elements in other domains is reduced to find the minimum requirement. The analysis was undertaken with four different mesh grids: Normal (119,332 elements), Fine (169,803 elements), Finer (223,015 elements) and Extremely Fine (284,911) grids. This grid independency analysis procedure is based on [52,53]. Then, the fluid temperature and pile thermal storage among the models are compared. Since results from the Fine, Finer and Extremely Fine grids are almost the same (less than 0.003 °C difference in average fluid temperature and 1.3 kJ/m^3 difference in thermal energy stored in the thermal storage piles), this work selects the Finer mesh for the numerical models. The number of elements is reduced to 208,100 elements to keep the same element density when pile spacing is reduced.

2.6. Parametric analysis

Considering the observations of the first simulation and previous studies on energy structures with PCM, a parametric analysis was conducted to observe how different parameters impact the performance of the underground heat exchanger system with the Thermal Storage Piles. The parameters considered are the pile spacing (P_s - in terms of the screw pile helix diameter D), the ground thermal conductivity (λ_g), the PCM phase change temperature (T_{pc}) and the GSHP operational scheme. Both P_s and λ_g may influence the heat exchange between the EP and the TSP, thus affecting the GSHP performance and the underground thermal storage.

Furthermore, previous studies on single boreholes and piles debated the importance of the T_{pc} of the PCM [21,26], defining that the value should be the average between the undisturbed soil temperature and the fluid peak temperature to obtain maximum GSHP performance. However, here the PCM location is fairly distant from the energy pile in comparison to the referred works. Therefore, instead of defining T_{pc} based on the fluid temperature, the T_{pc} adopted in each simulation is the average temperature of the TSPs during the simulated year, which is expected to maximise the utilisation of the latent heat. In addition, an evaluation considering mixing two different T_{pc} in different piles is undertaken, aiming for a longer and smoother phase change process of the PCM, which is expected to improve heat exchange [54]. Last, different operational schemes of the GSHP are considered to evaluate how the thermal load impacts the system performance. Table 2 presents a summary of the different parameters considered in the different scenarios.

Each scenario consists of a combination of the parameters presented in Table 2. In order to isolate the influence of the PCM on the GSHP performance and thermal storage in each scenario, two cases were considered: one where the TSPs are filled with air (i.e., empty – hereafter Reference case) and another one where the PCM replaces the air inside the TSPs (PCM case). The analyses use comparison metrics (Eq. (15) and (16)) based on the average fluid temperature in the pipes (T_f) and the heat pump CCOP and HCOP (and the resulting average monthly COP). Regarding thermal storage, no comparison metric is required since the piles with air store nearly zero heat energy. The resulting fluid temperatures, CCOP and HCOP from the simulations are presented in Appendix A, as the analyses focus mainly on the comparison between Reference and PCM cases of each different scenario, defined by the following metrics.

$$T_{f,diff} = T_{f,PCM} - T_{f,Ref} \tag{15}$$

$$COP_{change} = \frac{COP_{PCM}}{COP_{Ref}} - 1 \tag{16}$$

where *Ref* stands for the Reference case and *PCM* for the PCM case. Therefore $T_{f,diff}$ is the difference of average fluid temperatures between both cases in °C, and COP_{change} is the percentage that the COP in the PCM case increases or decreases in comparison to the Reference case.

3. Results and discussion

3.1. Model validation

The inlet fluid temperature recorded in the experimental work from Mousa and coworkers [25] was used as an input to the numerical model in this work, and the validation was undertaken by comparing experimental and numerical results of the outlet fluid temperature and the temperature recorded mid-depth in the PCM container. The outlet fluid temperature from the numerical simulation and experiment has great agreement, as shown in Fig. 6a. Since the horizontal location of the temperature sensor in the experiment was not clarified in the referred work, the temperature calculated from our numerical model at both the centre and on the edges at mid-depth of the container were used for validation (green and blue lines in Fig. 6b). The numerical result at the

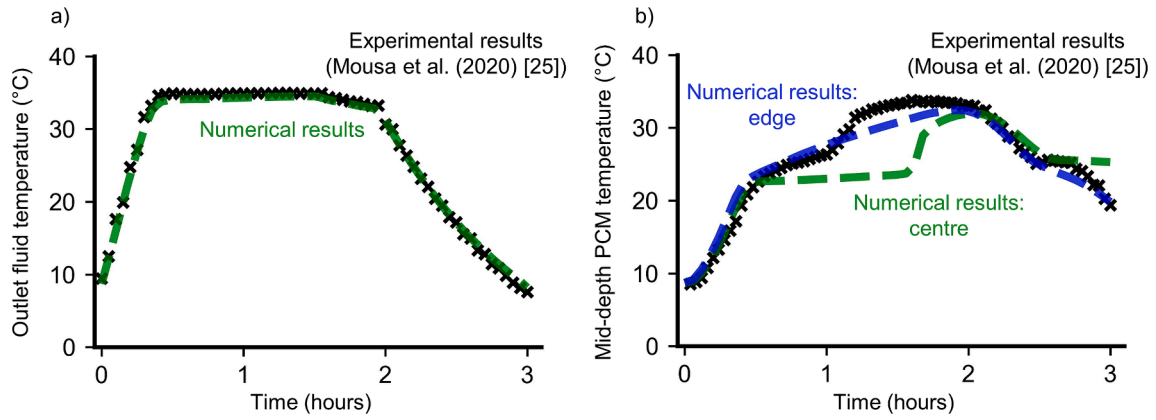

Fig. 6. Comparison of numerical and experimental results of outlet fluid temperature (a) and PCM temperature (b) for validation of the model.

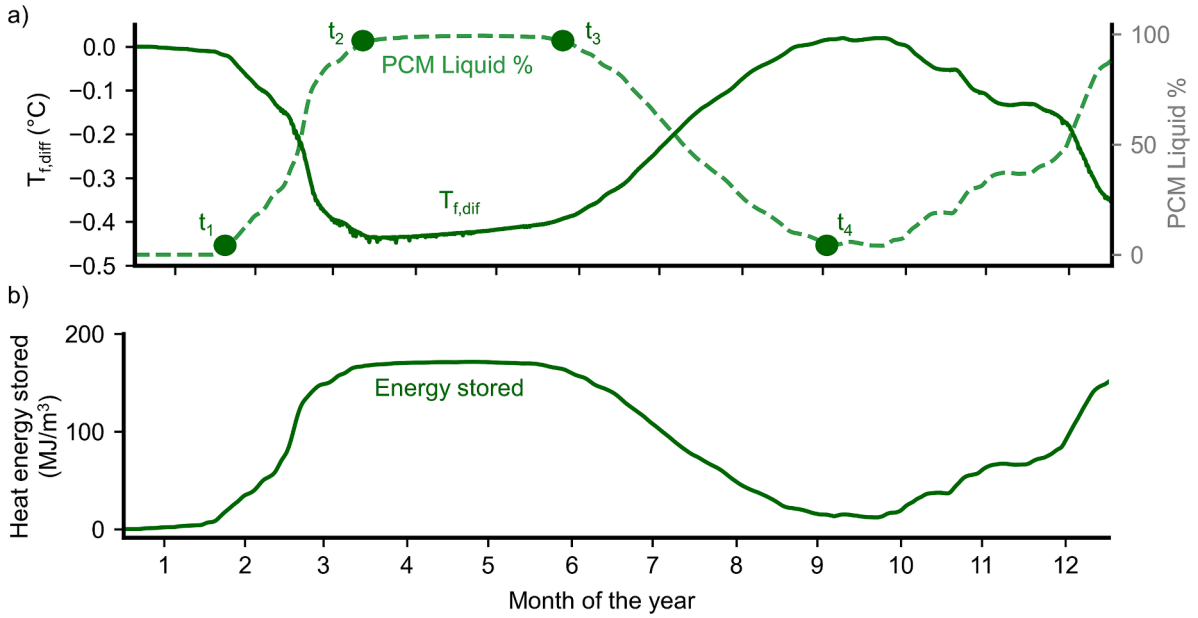

Fig. 7. $T_{f,diff}$ and PCM liquid phase percentage (a) and heat stored in the neighbour piles with PCM (b) over the whole simulation, considering $P_s = 3 \bullet D$ and $\lambda_g = 1.5$ W/(m•K).

centre of the container was taken from a point measurement and the temperature is constant during the phase change, while the result on the edge of the container is an average value over the inside perimeter of the PCM container. Hence, the latter presents a better fit against the experimental measurements. The work by Mousa and others [25] also conducted a numerical simulation validated by their experimental results. Similar to their observations, the agreement for the outlet fluid temperature (Fig. 6a) is greater than the temperature in the PCM container (Fig. 6b).

3.2. EP and TSP operation

The analysis of the energy screw pile model considered a pile spacing of 1.05 m (three times the helix diameter D) which is the lower limit to avoid reduction of the individual pile support capabilities due to group effects [55,56] and neighbour installation disturbances [57]. Considering the scenario with the full (scaled) thermal load from Fig. 4 and the remaining input parameters from Table 1, the average temperature of the TSPs is 24 °C in the Reference case, hence the T_{pc} value of the PCM inserted in the TSPs was set to the same 24 °C in the PCM case. The solid and dashed lines in Fig. 7 a present the $T_{f,diff}$ over time and the corresponding PCM liquid state percentage for the whole year, respectively.

Four key moments of the simulation are marked in Fig. 7 a: when the PCM started to melt for the first time (t_1 – liquid share is 5 %); when the PCM was fully melted (t_2 – liquid share reaches 95 %); when the PCM started to solidify for the first time (t_3 – liquid share drops back to 95 %) and when the PCM was back to solid state (t_4 – liquid share reaches 5 % again). The fluid temperature difference $T_{f,diff}$ started to decrease considerably (i.e., the fluid temperature in the PCM case is lower/cooler than in Reference) when the PCM started to melt (t1), as a substantial share of the heat rejected in the soil was absorbed by the PCM during the cooling operation. After the PCM was fully melted at t_2, $T_{f,diff}$ stabilizes until t_3 (6th month – June) when the winter operation of the heat pump absorbed the heat from the underground and the PCM released energy and started solidification, hence the value of $T_{f,diff}$ increased over three months until back to nearly zero (t_4). Subsequently, the warmer weather of the forthcoming summer season induced heat rejection into the ground by the GSHP, activating another round of PCM melting process. However, the impact of inserting the PCM in the TSP piles in the fluid temperature was minimal. $|T_{f,diff}|$ value did not rise above 0.5 °C, while the average fluid temperature value varied between 18 °C and 37.1 °C in

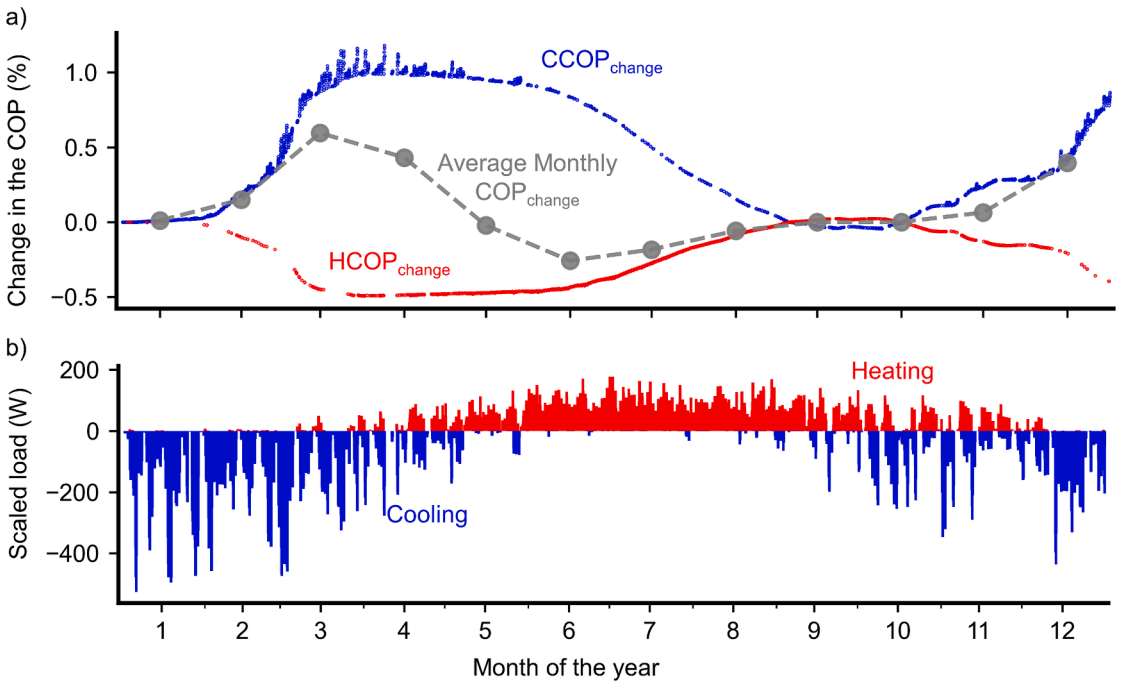

Fig. 8. COP change values for cooling, heating and monthly average (a), considering pile spacing = 3•D and λg = 1.5 W/(m•K), and the respective scaled thermal load for comparison (b).

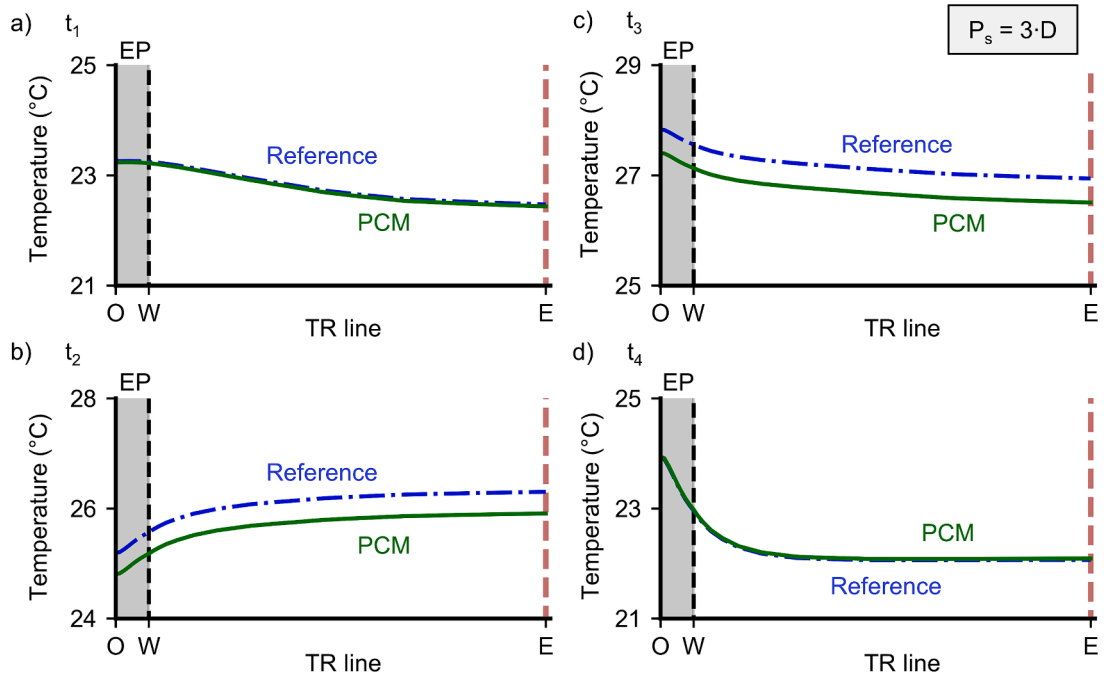

Fig. 9. Temperatures recorded in the energy pile and soil along the TR line, from the centre of the model (O) to the edge (E), at the instants t_1 (a), t_2 (b), t_3 (c) and t_4 (d) registered in Fig. 7. PCM and reference models with pile spacing = 3•D and λ_g = 1.5 W/(m•K).

the Reference case and 36.9 °C in the PCM case. Moreover, there was barely any visual hourly variation of $T_{f,diff}$ in Fig. 7, indicating that the PCM temperature did not respond in the short term to the variable thermal load and there was a delay between the heat rejected by the EP and the heat absorbed by the TSP. The most likely reason for this delayed response is the distance between the TSPs and the EP. Therefore, the PCM cools down the fluid temperature over several months (i.e., seasonal effect).

Fig. 7b presents the heat energy stored in the neighbour piles. The peak value is 171.4 MJ/m^3, mostly from the PCM latent heat storage (158.5 MJ/m^3). Comparatively, the same energy storage peak in the Reference case is 12.4 kJ/m3, negligible in comparison to the PCM case. This stresses the potential of using PCM with building foundations for underground thermal storage applications.

The lower fluid temperature resulting from the implementation of the PCM in the TSPs improved the CCOP of the heat pump. Fig. 8a presents the changes in both CCOP and HCOP caused by the implementation of the PCM in the TSPs, considering only the hours when

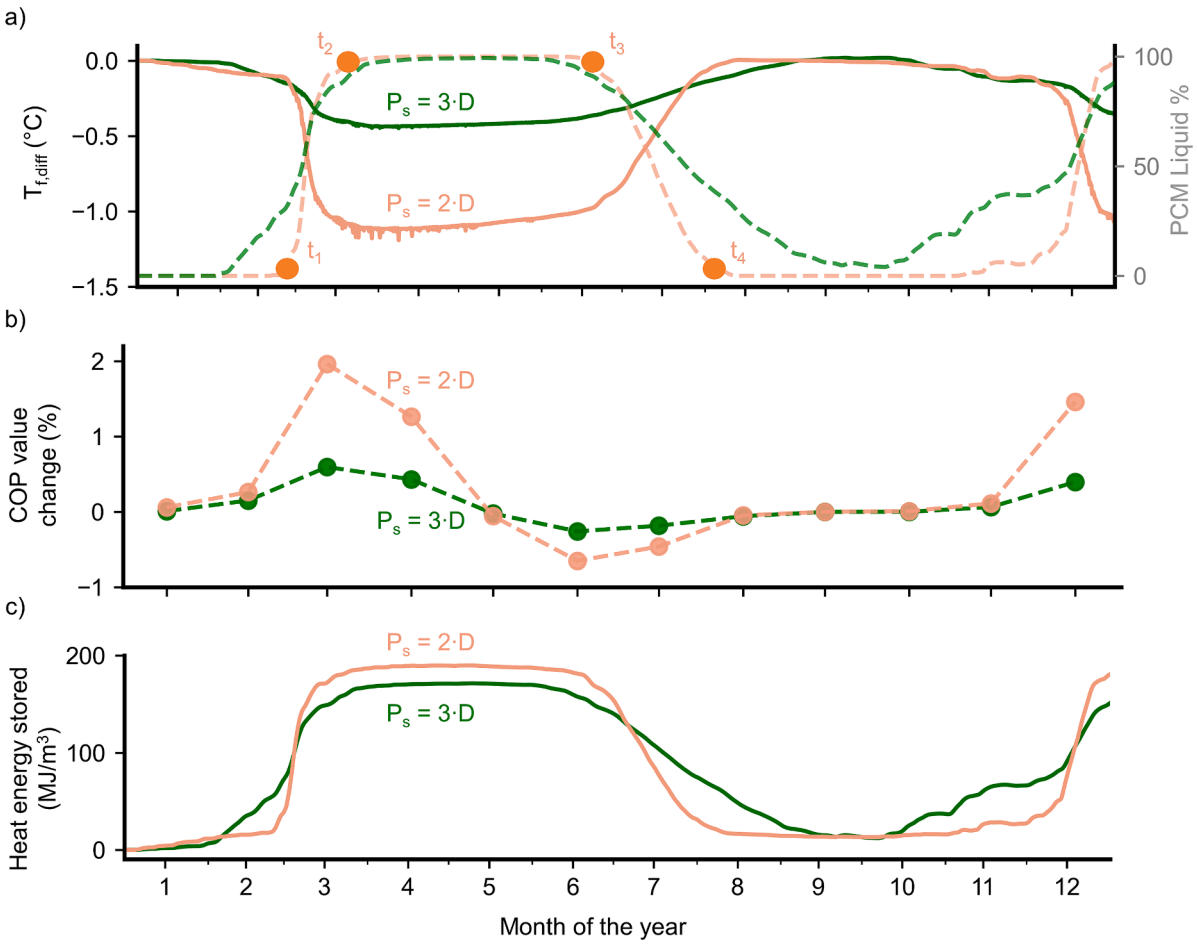

Fig. 10. $T_{f,diff}$ and PCM liquid phase percentage over time (a), Monthly average COP_{change} (b) and heat stored in the neighbour piles with PCM (c) over the whole simulation, for the models with P_s = 2•D and 3•D, considering λ_g = 1.5 W/(m•K).

either heating or cooling operation is active, and the respective monthly average considering changes in both CCOP and HCOP. The low fluid temperature difference reflected on small changes in the COPs, with a peak of 1.2 % increase of the $CCOP_{change}$ in early April. The lower fluid temperature of the PCM case increased $CCOP_{change}$ but decreased $HCOP_{change}$.

Despite the fact that the first couple of months of the year have a large cooling load, the late engagement of PCM latent heat (February - Fig. 7a) delayed the increase in the CCOP. By the end of March, the operation benefits from the higher CCOP. After that, the coming winter requires a heat-dominant thermal load, resulting in a lower HCOP and a sudden drop of average monthly COP_{change} to a negative value (i.e. the Reference case has a higher average COP). The winter operation ends in September so the PCM solidified again and the $T_{f,diff}$ is close to zero which means a similar COP from both Reference and PCM cases (i. e. COP_{change} is nearly zero). In October, the $CCOP_{change}$ started increasing again, so in the following year (not simulated) the PCM will be completely melted earlier, meaning a longer period of an advantageous CCOP for the PCM case during the next summer.

Another advantage of implementing the PCM in the TSPs is the reduction of the thermal radius and consequent reduction of pile-pile thermal interference. Fig. 9 shows the temperatures recorded by each case simulated (Reference and PCM) at the TR line (Fig. 3), where O is the centre of the EP, W is the EP wall and E is the model edge. Until the beginning of the phase change, there was no visual difference in either pile or ground temperature from each case and there is undergoing thermal interaction already (t_1 - Fig. 9a). After almost all of the PCM was melted (t_2 - Fig. 9b), the latent heat of the PCM reduced the soil temperature by 0.4 °C overall. The difference remains until the PCM started to melt again (t_3 - Fig. 9c) and was back to nearly zero when the PCM was back to a solid state (t_4 - Fig. 9d). In the PCM case, the energy stored in the neighbour piles by the PCM kept the soil temperature lower, so less heat interference happened between energy piles and more energy can be stored underground at the same temperature level than in the Reference case.

3.3. Parametric analysis results

3.3.1. Pile spacing

Even though the load capacity of the screw piles might be reduced due to group effects, a pile spacing (P_s) of less than 3•D may be required in a constrained space. The model geometry was adjusted by reducing P_s to 2•D (0.7 m). The shorter spacing resulted in higher thermal interaction and raised the overall temperature values. For this scenario, the average fluid temperature in the Reference case now increased to 46.4 °C at its peak. The average simulated temperature of the TSPs in the Reference case is now 32 °C, hence this was selected as the T_{pc} in the PCM case of this scenario with P_s = 2•D. Fig. 10a presents the impact of the new pile spacing on $T_{f,diff}$ and the PCM solid share in comparison to the previous simulations with 3•D. The $T_{f,diff}$ value was about three times lower during the peak difference period, from March to June. The lower $T_{f,diff}$ resulted in a higher CCOP and lower HCOP in the PCM case during these months, resulting in a greater change in the monthly average COP_{change} (Fig. 10b). The PCM in the model with shorter pile spacing experienced a later and quicker liquefaction, leading to higher energy storage (189.8 MJ/m^3 peak for 2•D spacing - Fig. 10c). In the

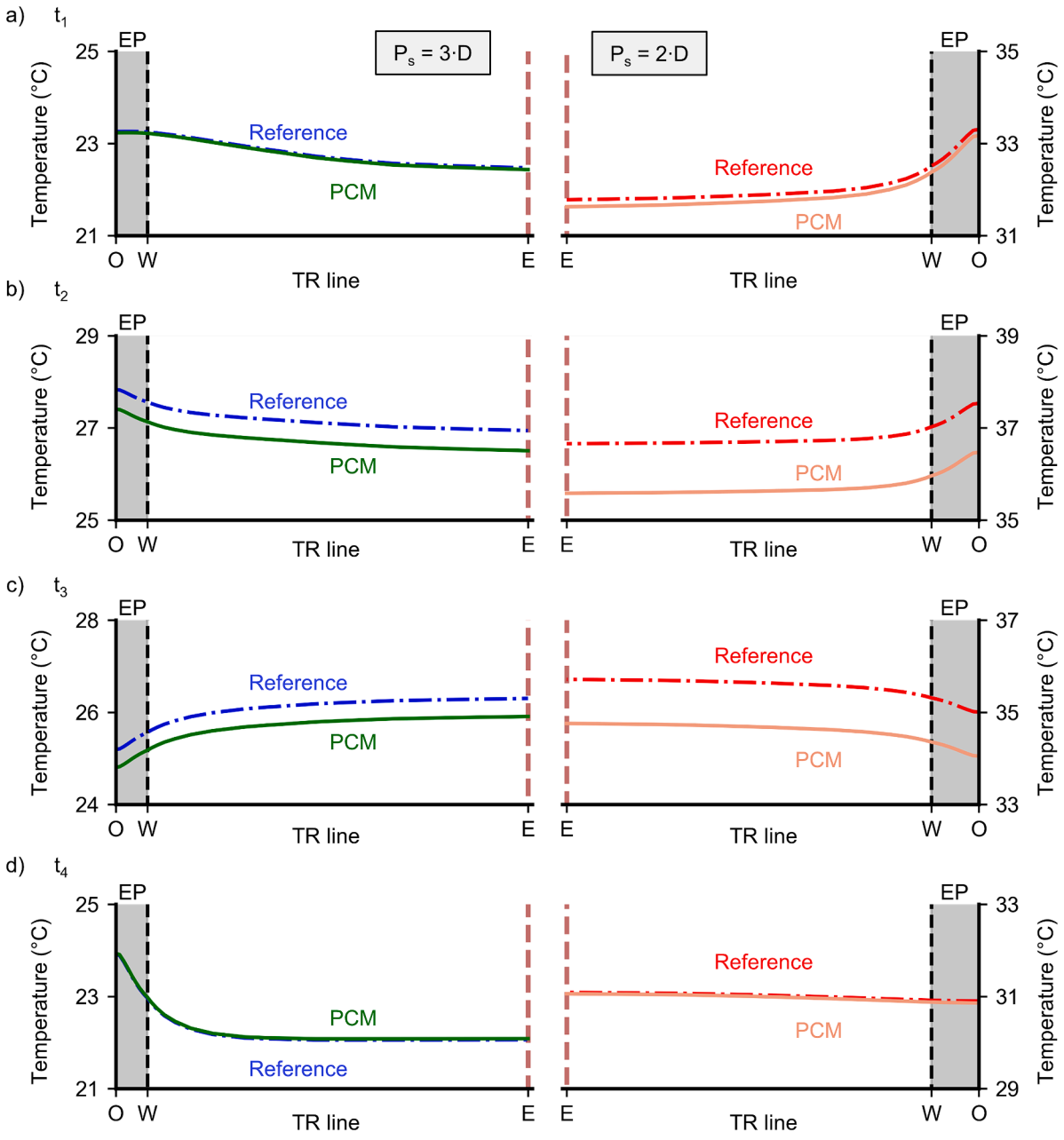

Fig. 11. Temperatures recorded in the energy pile (EP) and soil along the TR line in the models considering P_s = 3•D (left) and P_s = 2•D (right), both with λ_g = 1.5 W/(m•K), at the respective instants t_1 (a), t_2 (b), t_3 (c) and t_4 (d) registered in Fig. 9 and Fig. 10.

PCM cases, the TSPs' peak temperature is 39 °C for 2•D spacing and 27 °C for 3•D spacing. However, even with the distance reduction between the EP and the TSPs, there was still no short-term response of the PCM (i.e., no significant hourly variation of the $T_{f,diff}$ or the PCM solid share) and the $T_{f,diff}$ remained steady over several months. If the PCM could be engaged in the short term, the increased heat exchange during phase change would decrease $T_{f,diff}$ further, which would increase COP_{change} and potentially increase the advantage of implementing the PCM.

The smaller pile spacing led to greater thermal interference between EPs; however, the PCM reduced the soil temperature by a larger margin in the short spacing scenario. Fig. 11 presents the soil and pile temperatures along the TR line in different moments of the simulation scenario with P_s = 2•D (t_1, t_2, t_3 and t_4 from Fig. 10) mirrored against the scenario with P_s = 3•D (as presented in Fig. 9) for comparison. Again, O is the centre of the EP, W is the EP wall and E is the model edge. On the respective instants t_1 and t_4 (Fig. 11a and d), when the PCM was at a solid state, the temperature was the same in both Reference and PCM cases regardless of the spacing considered. However, when the latent heat was mobilised (instants t_2 and t_3 - Fig. 11b and c), the soil and pile temperatures are approximately 1 °C lower in the PCM case in comparison to the Reference case for P_s = 2•D, more than two times de difference observed for P_s = 3•D. The impact of the PCM was greater because it represented a larger fraction of the domain in the model with P_s = 2•D. Overall, the temperatures were higher in the scenarios with P_s = 2•D because the soil volume in the model was smaller but the thermal load rejected/extracted was the same.

3.3.2. *Mixed PCM phase change temperatures*

Considering that PCM energy screw piles perform higher heat exchange during the phase change process of the material [31], the implementation of PCMs with two different T_{pc} values was tested. Based

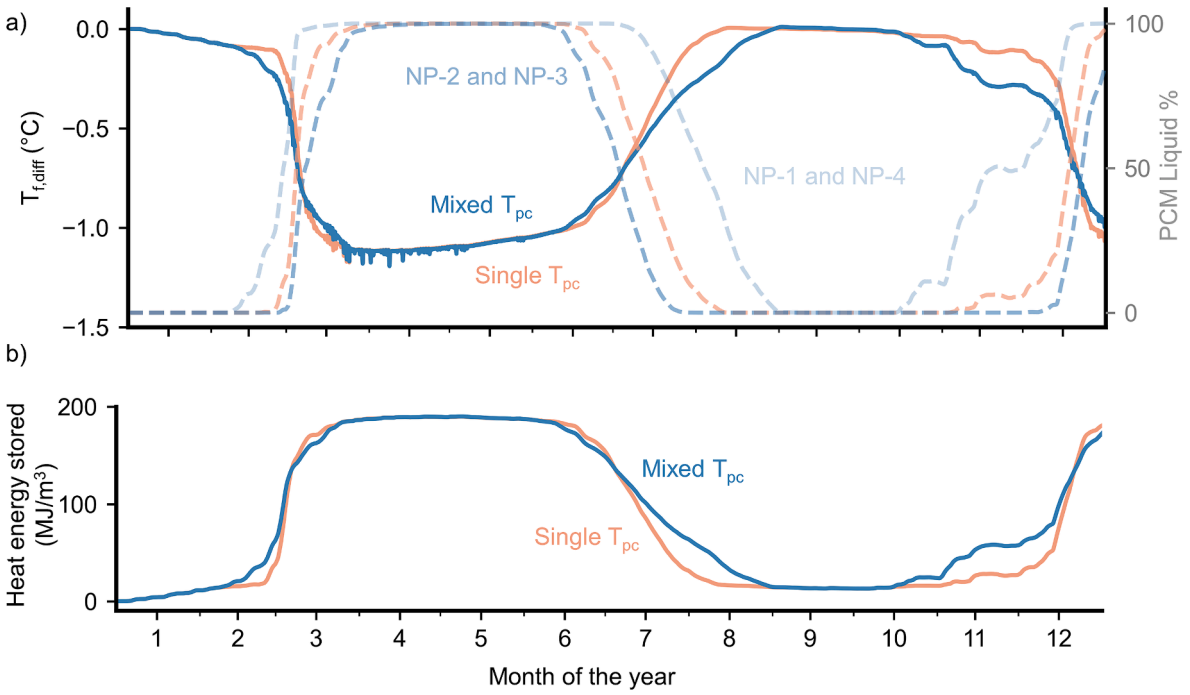

Fig. 12. $T_{f,diff}$ and PCM liquid percentage (a) and heat stored in the neighbour piles with PCM (b) over the whole simulation, for the models with Single and Mixed T_{pc} values, considering P_s = 2•D and λ_g = 1.5 W/(m•K).

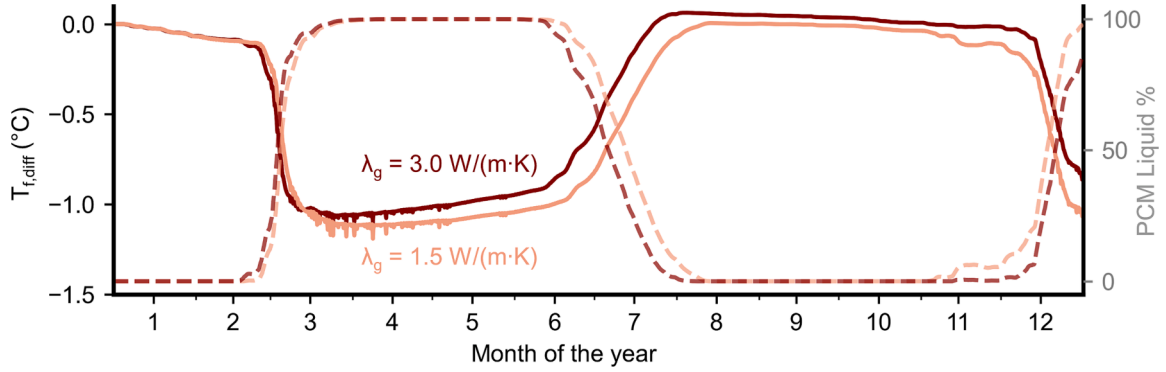

Fig. 13. $T_{f,diff}$ and PCM liquid percentage over time, for the models λ_g = 1.5 W/(m•K) and λ_g = 3.0 W/(m•K), considering P_s = 2•D.

on the model presented in Section 3.3.1, with piles spaced by P_s = 2•D and λ_g = 1.5 W/(m•K), the T_{pc} of 32 °C for all TSPs (Single T_{pc} value - Table 2) was replaced with 31 °C for the piles TSP1 and TSP4 and 34 °C for piles TSP2 and TSP3 (Mixed T_{pc} values - Table 2).

Fig. 12a) shows a smoother change of the $T_{f,diff}$ during the simulation time in the Mixed scenario in comparison to the Single one, with no changes of extreme values. The smother change happened because the phase change started earlier (in NP1 and NP4) and finished later (in NP2 and NP3). Different from the aforementioned studies from Section 1 [26,31], the PCM was not in direct contact with the heat exchanger pipes, thus the heat transport from the pipes to the PCM was delayed by its travel through the soil. Since the $T_{f,diff}$ of the Mixed T_{pc} and Single T_{pc} scenarios were similar and the COP is obtained from the fluid temperature, the COP of both scenarios are alike. Consequently, there were no noticeable changes to the COP_{change} value from Fig. 10b), hence it is not replicated in Fig. 12. Noting that the PCM latent heat was fully consumed in both scenarios, the heat storage over the year was also similar in both scenarios (Fig. 12b). Therefore, in the scenarios considered in this work, the use of PCMs with two different values of T_{pc} or a single value in the TSPs of the system resulted in the same improvement in performance.

3.3.3. Thermal conductivity

So far, the impact of implementing PCM in the TSPs was limited to a fairly constant $T_{f,diff}$ over the period of months, even though the thermal load changes every hour. Considering that a quicker heat exchange between the EP and the TSPs could result in a more intense use of the PCM, hence increase $T_{f,diff}$ variation, a scenario where the λ_g is increased by 100 % (from 1.5 W/(m•K) to 3.0 W/(m•K)) was considered in the parametric analysis, considering P_s = 2•D. On both scenarios, the average temperature in the TSPs was close to 32 °C, so the T_{pc} of the PCM was the same for both. Fig. 13 shows the $T_{f,diff}$ value over time and the PCM liquid percentage of both compared scenarios.. The $T_{f,diff}$ value was slightly higher for λ_g = 3.0 W/(m•K) after March, likely because the soil with a higher thermal conductivity can reject heat faster, meaning the axial heat transfer in both Reference and PCM cases was higher. Since more heat was transferred into the soil, the impact of implementing the PCM in the TSPs was lower (i.e. lower $|T_{f,diff}|$) when λ_g = 3.0 W/(m•K). Nevertheless, the observed difference in $T_{f,diff}$ and in the liquid share of the PCM in Fig. 13 is minimal considering the considerable change in λ_g

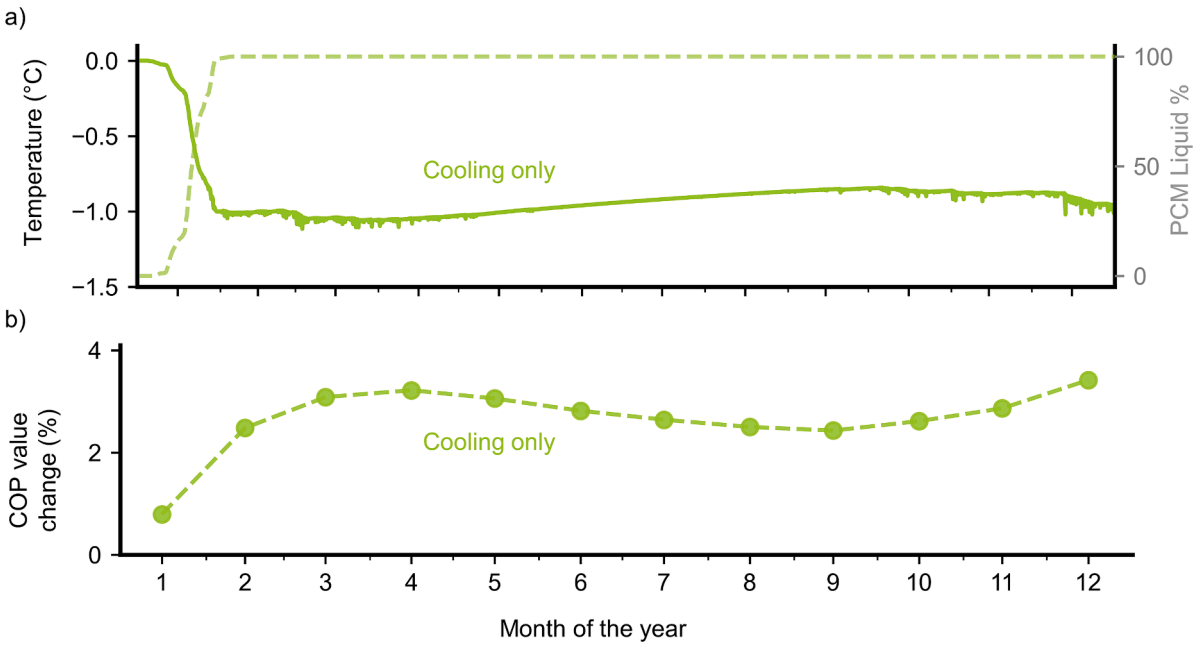

Fig. 14. $T_{f,diff}$ and PCM solid percentage over time (a) and Monthly average COP_{change} (b), for the models with $\lambda_g = 3.0$ W/(m•K) and $P_s = 2$•D with GSHP operating for cooling only (i.e., no heating thermal load).

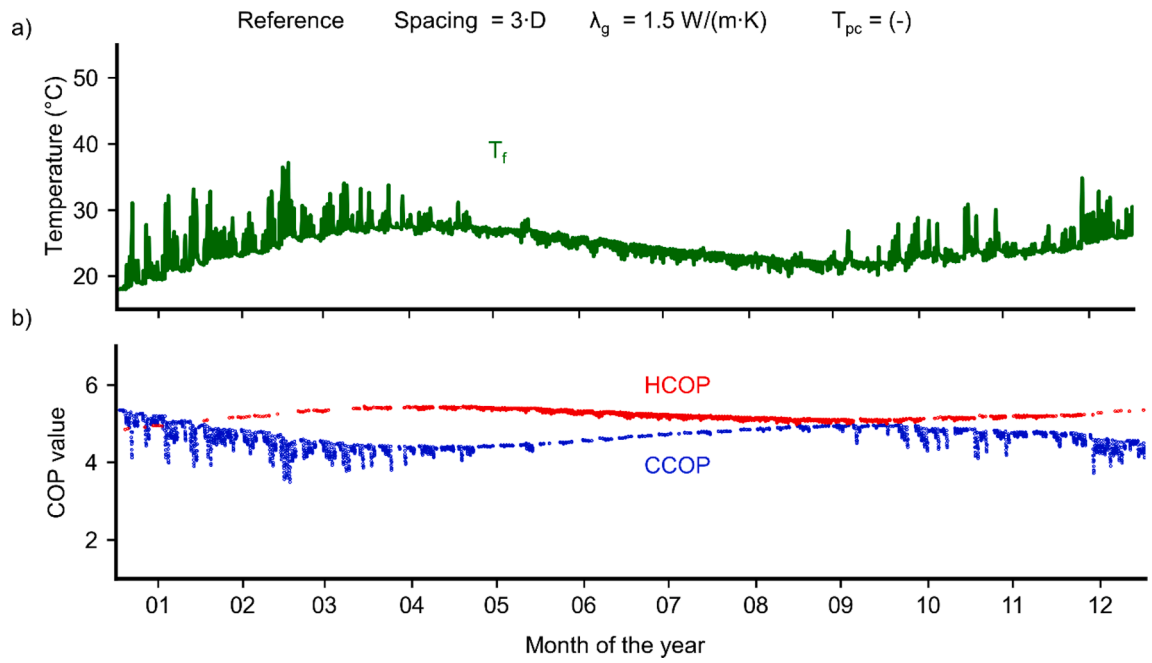

Fig. A1. Average fluid temperature (a) and CCOP and HCOP (b) values registered by the Reference case: Pile spacing = 3•D, $\lambda_g = 1.5$ W/(m•K), considering the full thermal load.

assessed in this analysis. It should be noticed that this work does not consider any groundwater flow, which would impact the dynamics of the thermal interactions between EP and TSPs.

3.3.4. Operational scheme

The previous simulations showed that implementing PCM in the TSPs benefits mainly the cooling performance of the GSHP in the cases studied herein. Therefore, the last part of this parametric analysis assessed the system response when only the cooling share of the thermal load is provided by the GSHP. Besides cooling only operation, this scenario considered $P_s = 2$•D and $\lambda_g = 3.0$ W/(m•K). Different from previous scenarios, the T_{pc} was arbitrarily set to 22 °C to ensure the PCM was 100 % solid when the simulation started, and latent heat was engaged as soon as possible. As shown in Fig. 14, the early start of the phase change led to a quick drop of $T_{f,diff}$ slightly below −1.0 °C in the first month, remaining fairly constant throughout the year (as the cooling only operation keeps the PCM at a liquid state). Although $T_{f,diff}$ did not drop much lower than other simulations with 2•D spacing, the benefits on the monthly average COP_{change} were greater because the lower HCOP of the PCM case was not considered (i.e. no heating operation - Fig. 14b). However, the temperature of the fluid rose above 50 °C by the end of the year, which is above the recommended value for the

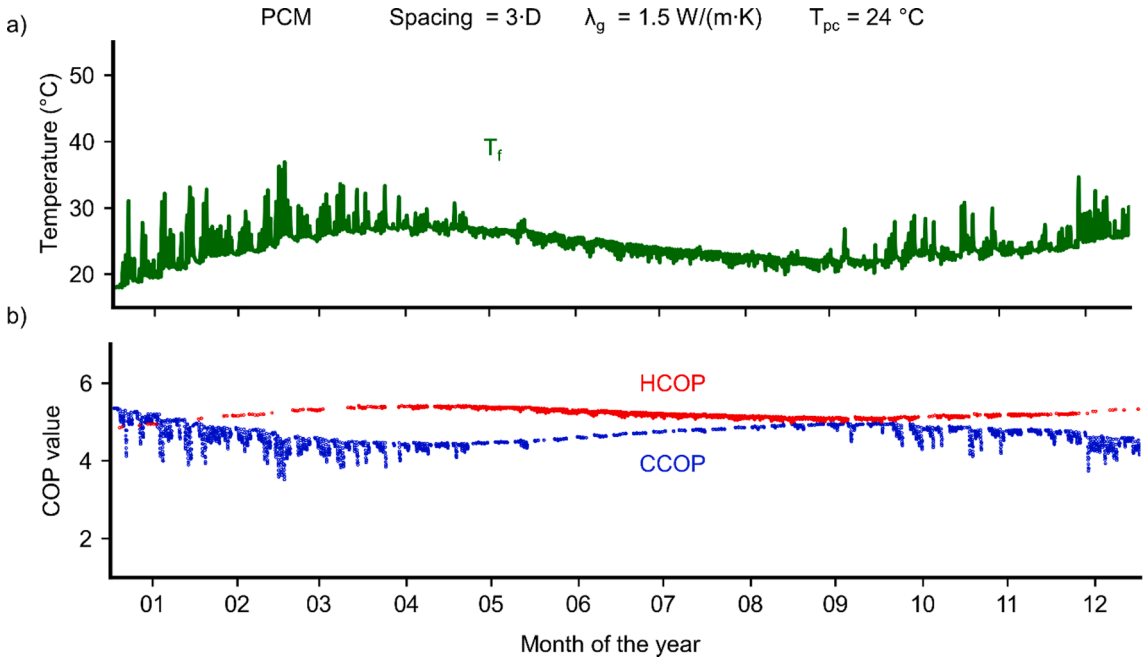

Fig. A2. Average fluid temperature (a) and CCOP and HCOP (b) values registered by the PCM case: Pile spacing = 3•D, λ_g = 1.5 W/(m•K), considering the full thermal load.

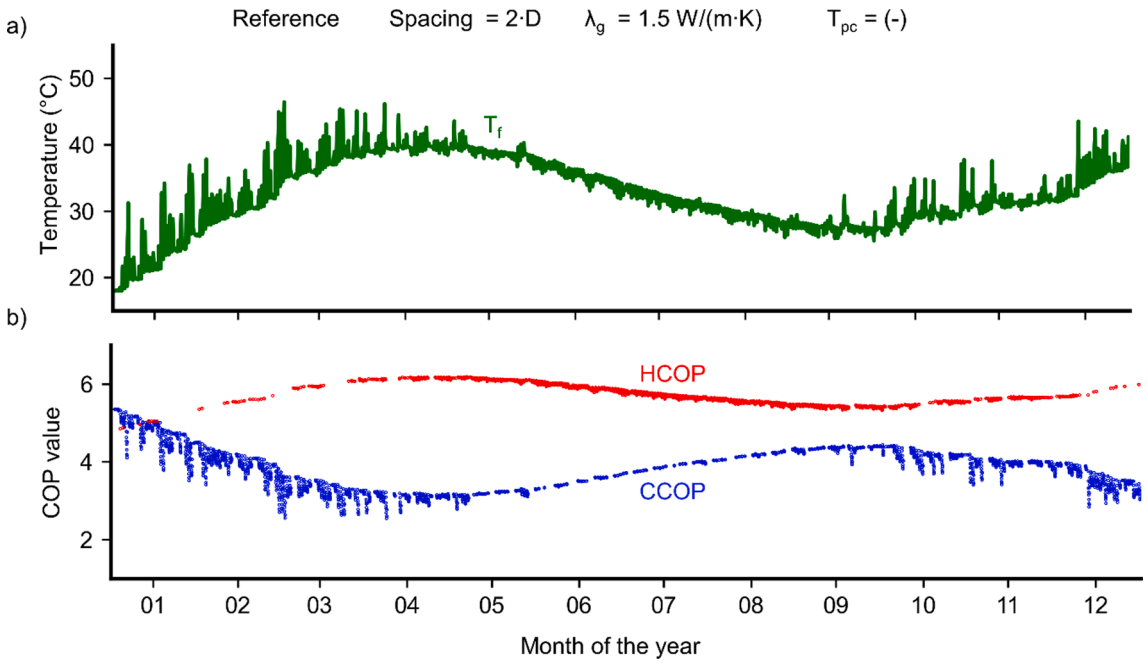

Fig. A3. Average fluid temperature (a) and CCOP and HCOP (b) values registered by the Reference case: Pile spacing = 2•D, λ_g = 1.5 W/(m•K), considering the full thermal load.

heat pump. The design would require additional piles or ground heat exchangers (boreholes) to provide the thermal load without overheating the GSHP. Because the fluid temperature was lower in the PCM case, implementing the PCM in the TSPs would likely require less additional heat exchangers than the Reference case (i.e., by employing the PCM inside the TSPs, a lower total heat exchanger length is required by the GSHP).

3.3.5. *Comparison with similar studies*

Implementing the PCM in the screw pile as a thermal storage pile instead of surrounding the HDPE pipes in the energy screw pile (Fei et al. (2023) [31]) eliminated the shortcoming related to the low thermal conductivity of the PCM that hindered the heat transfer rate from the HDPE pipe to the soil surrounding the piles. The fluid temperature in all scenarios using thermal storage piles in this work was lower than that in the reference case, while the fluid temperature in the cases using only PCM-filled energy screw piles was highly dependent on the thermal conductivity of the filling material. The new system in this work could also improve the heat pump COP by 4.7 % in a single day and an average of 3.4 % in a month. These results are similar to what was observed by [26] (5.2 % maximum COP increase), who considered PCM containers inside a large concrete pile. In addition, utilising multiple PCM materials

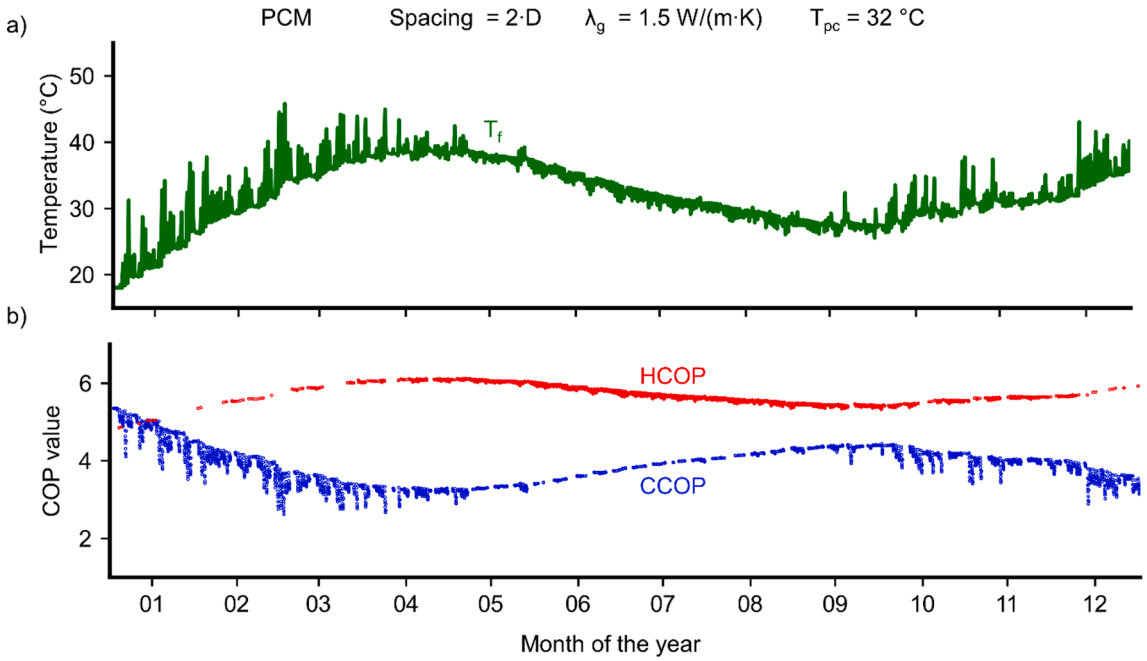

Fig. A4. Average fluid temperature (a) and CCOP and HCOP (b) values registered by the PCM case: Pile spacing = 2•D, λ_g = 1.5 W/(m•K), considering the full thermal load.

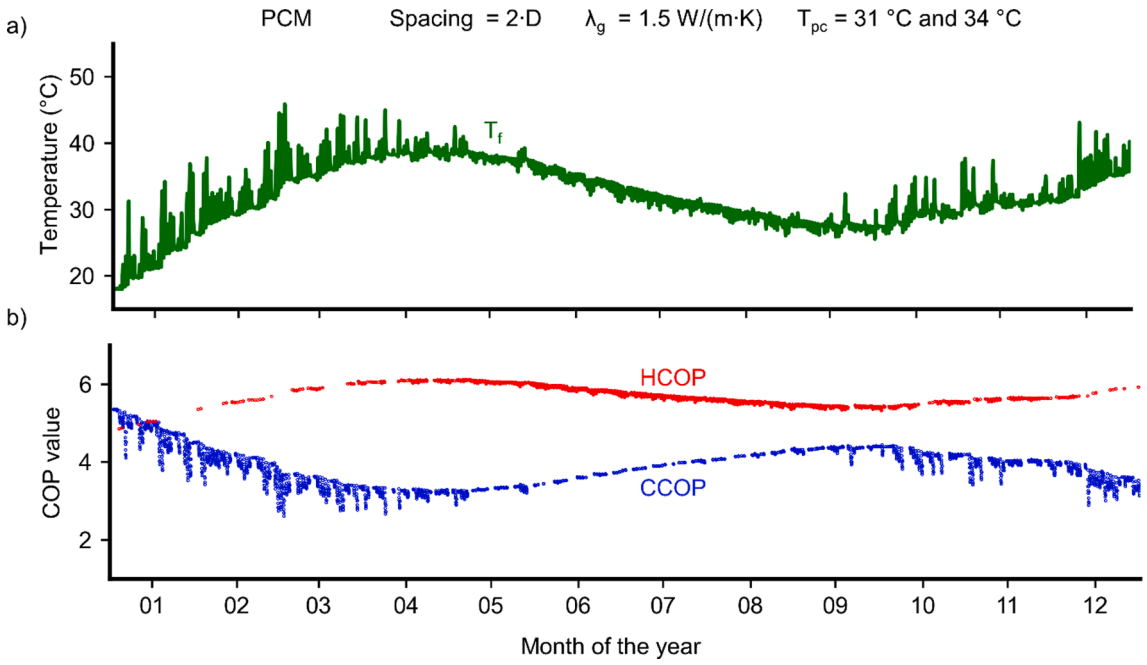

Fig. A5. Average fluid temperature (a) and CCOP and HCOP (b) values registered by the PCM case: Pile spacing = 2•D, λ_g = 1.5 W/(m•K), considering mixed T_{pc} values and the full thermal load.

with different T_{pc} values inside a single large concrete pile can lead to a significantly high COP increase, 15.1 % and 29.3 % reported in [26] and [27], respectively. However, considering multiple PCM materials in different TSPs did not produce a similar effect in the simulations performed in this work. It is noticeable that both aforementioned studies consider a different foundation solution (large diameter concrete cast-in-place piles) with different limitations when implementing the PCM.

4. Summary and conclusions

This work presented a new approach on the utilisation of Phase Change Materials in combination with energy screw piles for underground thermal storage and shallow geothermal systems. The proposed system utilises a large number of previously idle screw piles for thermal storage by filling them with Phase Change Materials (Thermal Storage Pile), while the remaining screw piles are connected to a Ground Source Heat Pump and act as traditional pile heat exchangers (Energy pile). A numerical model was used to analyse the performance of the heat pump

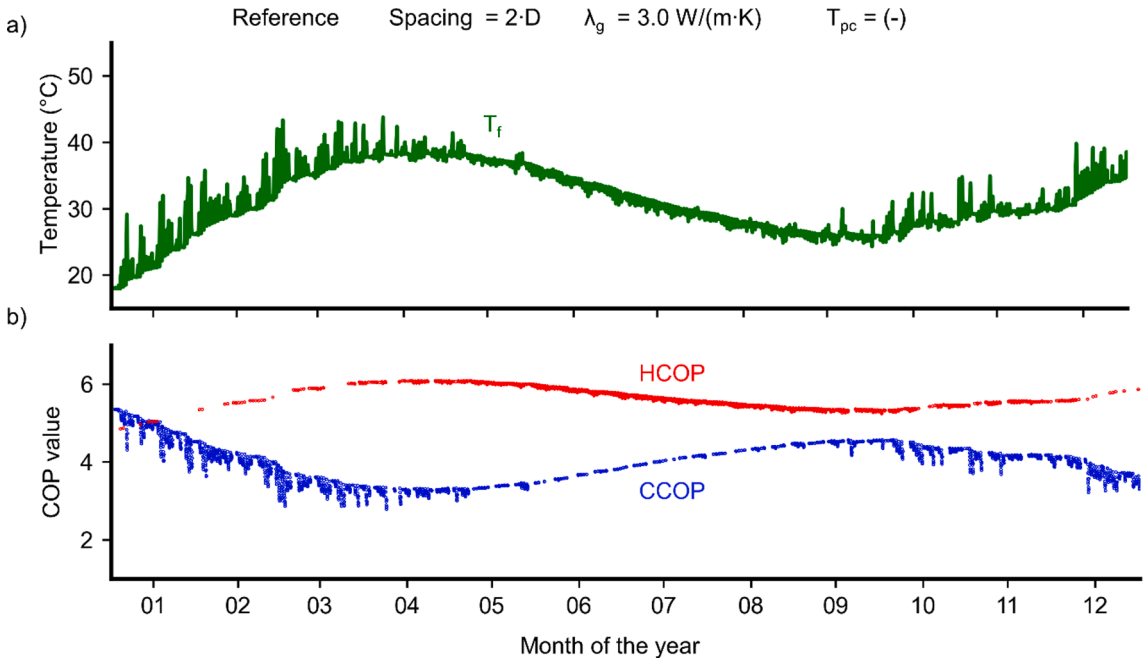

Fig. A6. Average fluid temperature (a) and CCOP and HCOP (b) values registered by the Reference case: Pile spacing = 2•D, λ_g = 3.0 W/(m•K), considering the full thermal load.

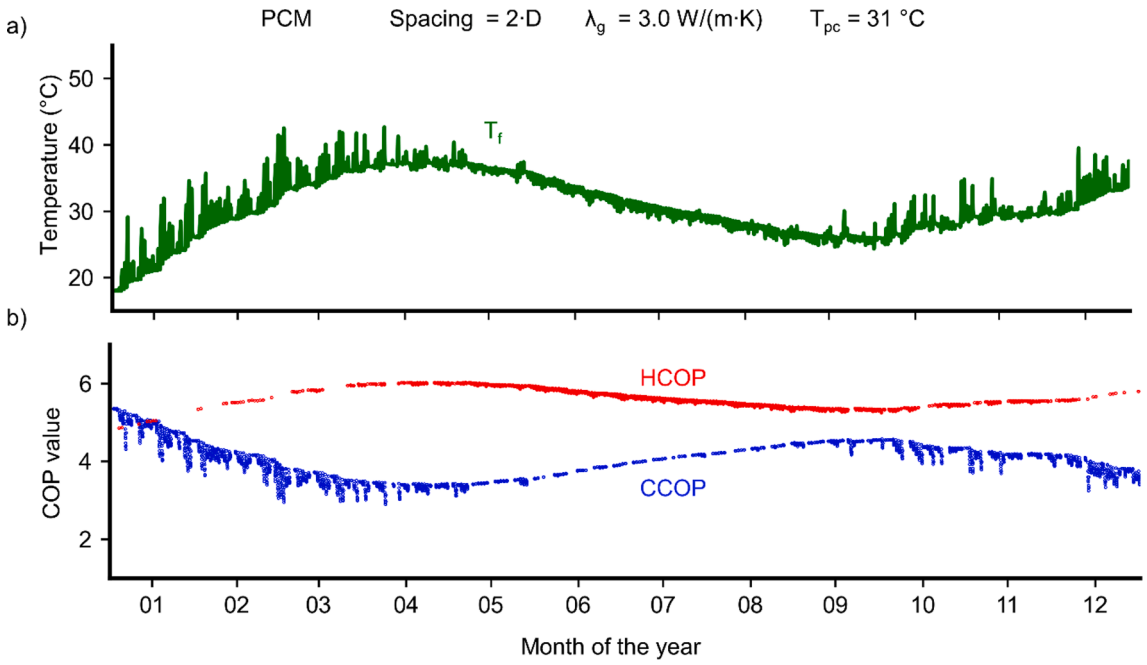

Fig. A7. Average fluid temperature (a) and CCOP and HCOP (b) values registered by the PCM case: Pile spacing = 2•D, λ_g = 3.0 W/(m•K), considering the full thermal load.

and the thermal storage capacity caused by the use of the Phase Change Material in the new system. Moreover, a parametric analysis was conducted to evaluate the performance of the system under different scenarios. Here are a few of the lessons obtained:

- The proposed system improved the performance of the heat pump in all scenarios that were considered. The implementation of the Phase Change Materials outside the energy screw pile was successful in bypassing the reduction of the heat exchange rate caused by the low thermal conductivity of the Phase Change Material reported in the literature. However, the increase in performance of the heat pump is minor, which might be because screw piles in this work are relatively small and can host a limited quantity of Phase Change Materials.
- Regarding the construction of the Thermal Storage Piles, minor labour cost is expected; the only extra task on top of the foundation construction (required for structural support of the building) and Ground Source Heat Pump system implementation is to pour the Phase Change Material inside screw piles. Therefore, the implementation cost of the system is mostly comprised of the cost of the Phase Change Material.

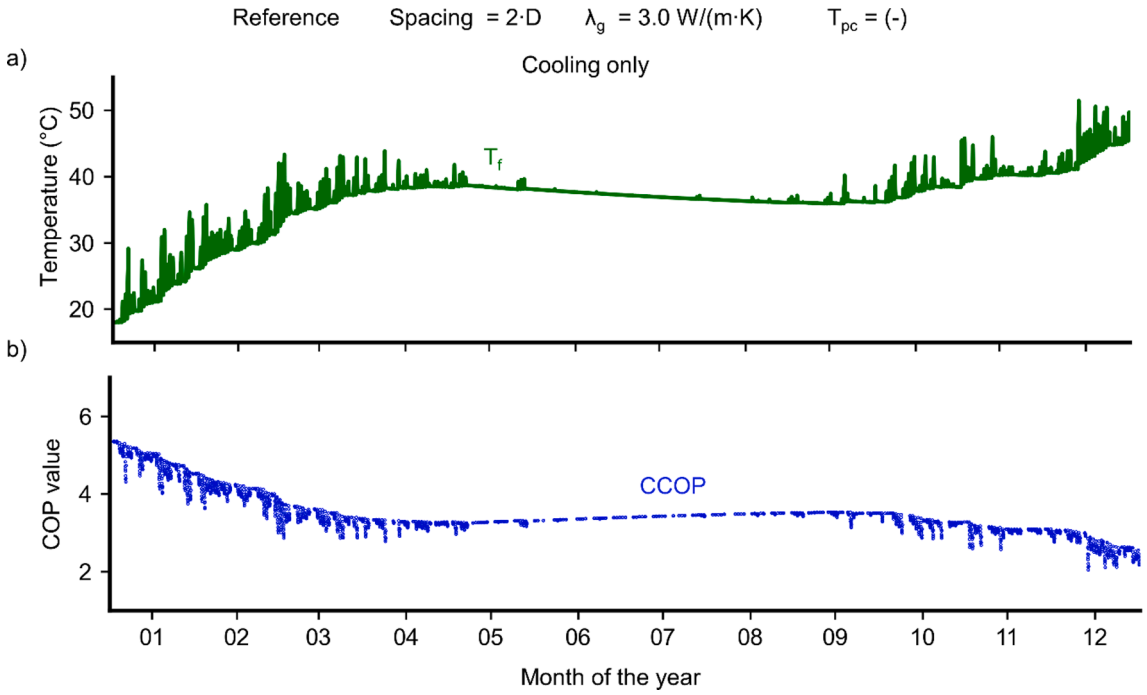

Fig. A8. Average fluid temperature (a) and CCOP and HCOP (b) values registered by the Reference case: Pile spacing = 2•D, λ_g = 3.0 W/(m•K), considering the cooling thermal load only.

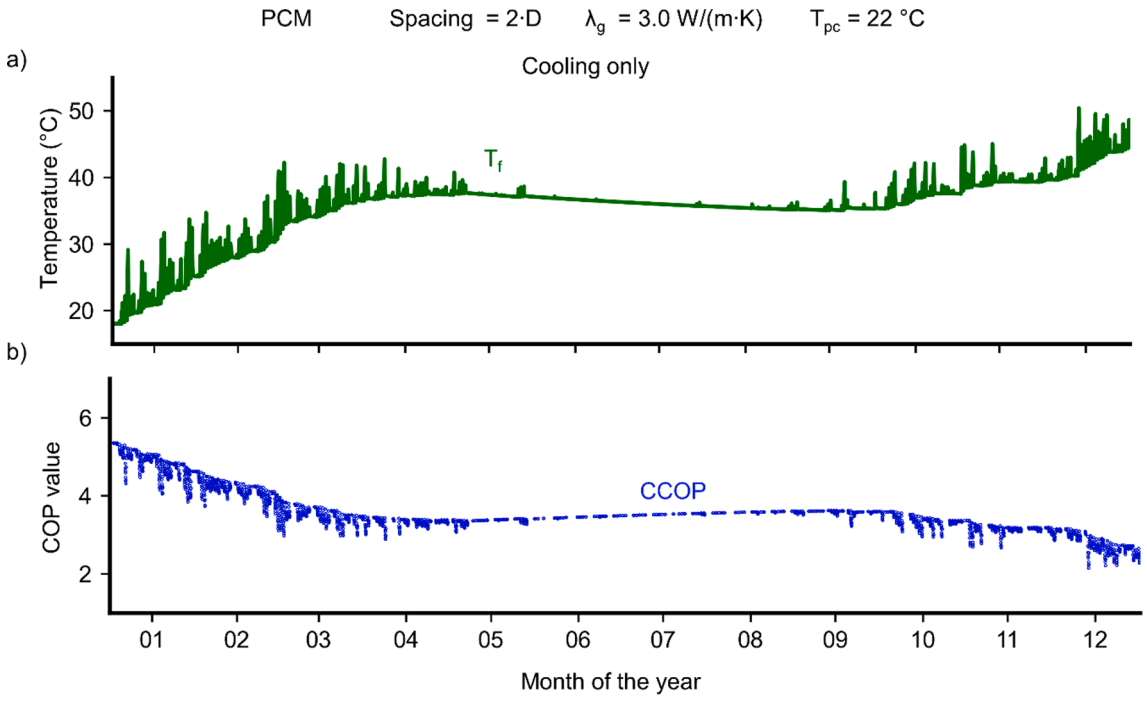

Fig. A9. Average fluid temperature (a) and CCOP and HCOP (b) values registered by the PCM case: Pile spacing = 2•D, λ_g = 3.0 W/(m•K), considering the cooling thermal load only.

- As observed in the literature [26,27], introducing Phase Change Materials into underground heat exchanger systems benefits one operation mode to the detriment of the other (Heating or Cooling). Consequently, the largest change in fluid temperatures and heat pump COP caused by the Phase Change Material in Thermal Storage Piles was observed when the cooling-only operational scheme is considered.
- The Phase Change Material phase change process occurs in a continuous and steady mode because of the distance between the heat exchanger and the Phase Change Material, even though the thermal load considered in the simulation has abrupt hourly variations. Moreover, parametric analysis shows that pile spacing had the second largest impact on the system performance increase caused by the Phase Change Material. However, considering the characteristics of screw pile foundations, it is highly unlikely that the spacing

between screw piles would be lower than two times the helix diameter. Meanwhile, the soil thermal conductivity and the phase change temperature of the material had a negligible impact on the fluid temperature and coefficient of performance, different from what is observed in other studies [21,26,31].

- Although not evaluated in this work, the combination of Energy Piles and Thermal Storage Piles can be implemented for Thermal Energy Storage (TES) applications [58–60], given its relatively simple implementation. However, the system should be evaluated under specific operations and metrics to assess its efficiency and feasibility.

Declaration of Competing Interest

The authors declare that they have no known competing financial interests or personal relationships that could have appeared to influence the work reported in this paper.

Data availability

Data will be made available on request.

Acknowledgments

The authors acknowledge the Early Career Research Grant (2022ECR085) and 2022 CIS-IE Seed Funding provided by the University of Melbourne and the Linkage Project (LP160101486) provided by the Australian Research Council. This research was supported by the use of the Nectar Research Cloud (collaborative Australian research platform supported by the NCRIS-funded Australian Research Data Commons), the University of Melbourne's Research Computing Services and the Petascale Campus Initiative Assistance in the computational analysis.

Appendix A. Model results

This appendix presents the average fluid temperature, CCOP and HCOP obtained in all 9 scenarios considered in this work (see Figs. A1–A9).

References

[1] M.J. Brown, C. Davidson, B. Cerfontaine, M. Ciantia, J. Knappett, A. Brennan, Developing screw piles for offshore renewable energy application, in: S. Haldar, S. Patra, R.K. Ghanekar (Eds.), Advances in Offshore Geotechnics, Springer Singapore, Singapore, 2020, pp. 101–119.
[2] G. Spagnoli, C.H.C. Tsuha, A review on the behavior of helical piles as a potential offshore foundation system, Mar. Georesour. Geotechnol. 38 (2020) 1013–1036, https://doi.org/10.1080/1064119X.2020.1729905.
[3] C.H.C. Tsuha, J.M.S. Mathias dos santos Filho, T.C. Santos, Helical piles in unsaturated structured soil: a case study, Can. Geotech. J. 53 (1) (2016) 103–117, https://doi.org/10.1139/cgj-2015-0017.
[4] L. Bandeira Neto, G. Narsilio, N. Makasis, R. Choudhary, Y. Carden, Thermal response of energy screw piles connected in series, J. Geotech. Geoenviron. Eng. 149 (2023) 04023049, https://doi.org/10.1061/JGGEFK/GTENG-11082.
[5] J. Huang, J.S. McCartney, H. Perko, D. Johnson, C. Zheng, Q. Yang, A novel energy pile: the thermo-syphon helical pile, Appl. Therm. Eng. 159 (2019), 113882, https://doi.org/10.1016/j.applthermaleng.2019.113882.
[6] Jalaluddin, A. Miyara, K. Tsubaki, S. Inoue, K. Yoshida, Experimental study of several types of ground heat exchanger using a steel pile foundation, Renew. Energy 36 (2011) 764–771, https://doi.org/10.1016/j.renene.2010.08.011.
[7] I.W. Johnston, G.A. Narsilio, S. Colls, Emerging geothermal energy technologies, KSCE J. Civ. Eng. 15 (2011) 643–653, https://doi.org/10.1007/s12205-011-0005-7.
[8] D. Adam, R. Markiewicz, Energy from earth-coupled structures, foundations, tunnels and sewers, Géotechnique 59 (2009) 229–236, https://doi.org/10.1680/geot.2009.59.3.229.
[9] Y. Rabin, E. Korin, Incorporation of phase-change materials into a ground thermal energy storage system: theoretical study, J. Energy Res. Technol. 118 (1996) 237–241, https://doi.org/10.1115/1.2793868.
[10] S. Bouckaert, A.F. Pales, C. McGlade, U. Remme, L. Varro, D. D'Ambrosio, T. Spencer, Net Zero by 2050: A Roadmap for the Global Energy Sector, IEA, Paris, 2021.
[11] M.C.F. Murari, C.H.C. Tsuha, F. Loveridge, Investigation on the thermal response of steel pipe energy piles with different backfill materials, Renew. Energy 199 (2022) 44–61, https://doi.org/10.1016/j.renene.2022.08.105.
[12] A. Fallahi, G. Guldentops, M. Tao, S. Granados-Focil, S. Van Dessel, Review on solid-solid phase change materials for thermal energy storage: molecular structure and thermal properties, Appl. Therm. Eng. 127 (2017) 1427–1441, https://doi.org/10.1016/j.applthermaleng.2017.08.161.
[13] Y. Konuklu, M. Ostry, H.O. Paksoy, P. Charvat, Review on using microencapsulated phase change materials (PCM) in building applications, Energ. Build. 106 (2015) 134–155, https://doi.org/10.1016/j.enbuild.2015.07.019.
[14] M. Zare, K.S. Mikkonen, Phase change materials for life science applications, Adv. Funct. Mater. 33 (2023), 2213455, https://doi.org/10.1002/adfm.202213455.
[15] I. Sarbu, C. Sebarchievici, A comprehensive review of thermal energy storage, Sustainability 10 (2018), 191.
[16] P.J. Shamberger, N.M. Bruno, Review of metallic phase change materials for high heat flux transient thermal management applications, Appl. Energy 258 (2020), 113955, https://doi.org/10.1016/j.apenergy.2019.113955.
[17] G. Gholamibozanjani, M. Farid, A comparison between passive and active PCM systems applied to buildings, Renew. Energy 162 (2020) 112–123, https://doi.org/10.1016/j.renene.2020.08.007.
[18] C. Li, X. Wen, W. Cai, H. Yu, D. Liu, Phase change material for passive cooling in building envelopes: a comprehensive review, J. Build. Eng. 65 (2023), 105763, https://doi.org/10.1016/j.jobe.2022.105763.
[19] F. Chen, J. Mao, S. Chen, C. Li, P. Hou, L. Liao, Efficiency analysis of utilizing phase change materials as grout for a vertical U-tube heat exchanger coupled ground source heat pump system, Appl. Therm. Eng. 130 (2018) 698–709, https://doi.org/10.1016/j.applthermaleng.2017.11.062.
[20] D. Cortes, A. Nasirian, S. Dai, Smart Ground-Source Borehole Heat Exchanger Backfills: A Numerical Study: SEG-2018, 2019, pp. 27–34, doi: 10.1007/978-3-319-99670-7_4.
[21] A. Aljabr, A. Chiasson, A. Alhajjaji, Numerical modeling of the effects of micro-encapsulated phase change materials intermixed with grout in vertical borehole heat exchangers, Geothermics 96 (2021), 102197, https://doi.org/10.1016/j.geothermics.2021.102197.
[22] P. Dehdezi, M. Hall, A. Dawson, Enhancement of soil thermophysical properties using microencapsulated phase change materials for ground source heat pump applications, Appl. Mech. Mater. (2011) 110–116, https://doi.org/10.4028/www.scientific.net/AMM.110-116.1191.
[23] M. Kong, J.L. Alvarado, C. Thies, S. Morefield, C.P. Marsh, Field evaluation of microencapsulated phase change material slurry in ground source heat pump systems, Energy 122 (2017) 691–700, https://doi.org/10.1016/j.energy.2016.12.092.
[24] W. Yang, B. Yang, F. Wang, N. Jing, Numerical evaluations on the effects of thermal properties on the thermo-mechanical behaviour of a phase change concrete energy pile, Energy Built Environ. (2021), https://doi.org/10.1016/j.enbenv.2021.05.008.
[25] M.M. Mousa, A.M. Bayomy, M.Z. Saghir, Experimental and numerical study on energy piles with phase change materials, Energies 13 (2020), 4699.
[26] M.M. Mousa, A.M. Bayomy, M.Z. Saghir, Long-term performance investigation of a GSHP with actual size energy pile with PCM, Appl. Therm. Eng. 210 (2022), 118381, https://doi.org/10.1016/j.applthermaleng.2022.118381.
[27] M. Alavy, M. Peiris, J. Wang, M.A. Rosen, Assessment of a novel phase change material-based thermal caisson for geothermal heating and cooling, Energ. Conver. Manage. 234 (2021), 113928, https://doi.org/10.1016/j.enconman.2021.113928.
[28] Z. Zhang, G. Shi, S. Wang, X. Fang, X. Liu, Thermal energy storage cement mortar containing n-octadecane/expanded graphite composite phase change material, Renew. Energy 50 (2013) 670–675, https://doi.org/10.1016/j.renene.2012.08.024.
[29] M. Hunger, A.G. Entrop, I. Mandilaras, H.J.H. Brouwers, M. Founti, The behavior of self-compacting concrete containing micro-encapsulated Phase Change Materials, Cem. Concr. Compos. 31 (2009) 731–743, https://doi.org/10.1016/j.cemconcomp.2009.08.002.
[30] X. Bao, S.A. Memon, H. Yang, Z. Dong, H. Cui, Thermal properties of cement-based composites for geothermal energy applications, Materials 10 (2017), 462.
[31] W. Fei, L.A. Bandeira Neto, S. Dai, D.D. Cortes, G.A. Narsilio, Numerical analyses of energy screw pile filled with phase change materials, Renew. Energy 202 (2023) 865–879, https://doi.org/10.1016/j.renene.2022.12.008.
[32] COMSOL, COMSOL Multiphysics v. 5.6, COMSOL AB, Stockholm, Sweden, 2021.
[33] F. Loveridge, W. Powrie, G-Functions for multiple interacting pile heat exchangers, Energy 64 (2014) 747–757, https://doi.org/10.1016/j.energy.2013.11.014.
[34] L.A. Bandeira Neto, G.A. Narsilio, N. Makasis, Analytical interpretation and numerical analysis of multiple energy pile thermal response tests, Comput. Geotech. 157 (2023), 105314, https://doi.org/10.1016/j.compgeo.2023.105314.
[35] A. Bidarmaghz, N. Makasis, W. Fei, G.A. Narsilio, An efficient and sustainable approach for cooling underground substations, Tunn. Undergr. Space Technol. 113 (2021), 103986, https://doi.org/10.1016/j.tust.2021.103986.
[36] X. Gu, N. Makasis, Y. Motamedi, G.A. Narsilio, A. Arulrajah, S. Horpibulsuk, Geothermal pavements: field observations, numerical modelling and long-term performance, Géotechnique (2021) 1–15, https://doi.org/10.1680/jgeot.20.P.296.
[37] A.F. Rotta Loria, A. Gunawan, C. Shi, L. Laloui, C.W.W. Ng, Numerical modelling of energy piles in saturated sand subjected to thermo-mechanical loads, Geomech. Energy Environ. 1 (2015) 1–15, https://doi.org/10.1016/j.gete.2015.03.002.
[38] A. Bidarmaghz, G.A. Narsilio, Shallow geothermal energy: emerging convective phenomena in permeable saturated soils, Géotechn. Lett. 6 (2016) 119–123, https://doi.org/10.1680/jgele.15.00167.

[39] S. Moench, R. Dittrich, Influence of natural convection and volume change on numerical simulation of phase change materials for latent heat storage, Energies 15 (2022), 2746.
[40] A. Bidarmaghz, 3D Numerical Modelling of Vertical Ground Heat Exchangers, Department of Infrastructure Engineering, The University of Melbourne, Melbourne, Australia, 2014.
[41] A. Bidarmaghz, N. Makasis, G.A. Narsilio, F.M. Francisca, M.E. Carro Pérez, Geothermal energy in loess, Environ. Geotechn. 3 (2016) 225–236, https://doi.org/10.1680/jenge.15.00025.
[42] A. Insana, M. Barla, Experimental and numerical investigations on the energy performance of a thermo-active tunnel, Renew. Energy 152 (2020) 781–792, https://doi.org/10.1016/j.renene.2020.01.086.
[43] A. Di Donna, L. Laloui, Numerical analysis of the geotechnical behaviour of energy piles, Int. J. Numer. Anal. Meth. Geomech. 39 (2015) 861–888, https://doi.org/10.1002/nag.2341.
[44] Y. Lu, D.D. Cortes, X. Yu, G. Narsilio, S. Dai, Numerical investigations of enhanced shallow geothermal energy recovery using microencapsulated phase change materials and metal fins, Acta Geotech. (2022), https://doi.org/10.1007/s11440-022-01715-1.
[45] Rubitherm Technologies GmbH, https://www.rubitherm.eu/en/productcategory/organische-pcm-rt, 2020 (accessed 1 September 2022).
[46] F. Agyenim, N. Hewitt, P. Eames, M. Smyth, A review of materials, heat transfer and phase change problem formulation for latent heat thermal energy storage systems (LHTESS), Renew. Sustain. Energy Rev. 14 (2010) 615–628, https://doi.org/10.1016/j.rser.2009.10.015.
[47] A. Trp, K. Lenic, B. Frankovic, Analysis of the influence of operating conditions and geometric parameters on heat transfer in water-paraffin shell-and-tube latent thermal energy storage unit, Appl. Therm. Eng. 26 (2006) 1830–1839, https://doi.org/10.1016/j.applthermaleng.2006.02.004.
[48] G. Li, Y. Hwang, R. Radermacher, Review of cold storage materials for air conditioning application, Int. J. Refrig. 35 (2012) 2053–2077, https://doi.org/10.1016/j.ijrefrig.2012.06.003.
[49] Y. Zhong, G.A. Narsilio, N. Makasis, C. Scott, Experimental and numerical studies on an energy piled wall: the effect of thermally activated pile spacing, Geomech. Energy Environ. 29 (2022), 100276, https://doi.org/10.1016/j.gete.2021.100276.
[50] G. Narsilio, A. Bidarmaghz, I. Johnston, Numerical Modelling of Ground Heat Exchangers with Different Ground Loop Configurations for Direct Geothermal Applications, 2013.
[51] CLIMATEMASTER, Tranquility Modular Water-to-Water (TMW) Heat Pump Series - Submittal set, Vol. 2023, 2023, https://www.climatemaster.com/3150.html#.
[52] G. Triscari, M. Santovito, M. Bressan, D. Papurello, Experimental and model validation of a phase change material heat exchanger integrated into a real building, Int. J. Energy Res. 45 (2021) 18222–18236, https://doi.org/10.1002/er.7037.
[53] F. Mohammadnejad, S. Hossainpour, A CFD modeling and investigation of a packed bed of high temperature phase change materials (PCMs) with different layer configurations, J. Storage Mater. 28 (2020), 101209, https://doi.org/10.1016/j.est.2020.101209.
[54] M.M. Mousa, A.M. Bayomy, M.Z. Saghir, Phase change materials effect on the thermal radius and energy storage capacity of energy piles: experimental and numerical study, Int. J. Thermofluids 10 (2021), 100094, https://doi.org/10.1016/j.ijft.2021.100094.
[55] A.S. Jamill, H.O. Abbas, Effect of screw piles spacing on group compressive capacity in soft clay, IOP Conf. Ser.: Mater. Sci. Eng. 1076 (2021), 012098, https://doi.org/10.1088/1757-899x/1076/1/012098.
[56] S.A. Lanyi-Bennett, L. Deng, Axial load testing of helical pile groups in glaciolacustrine clay, Can. Geotech. J. 56 (2019) 187–197, https://doi.org/10.1139/cgj-2017-0425.
[57] J.A. Schiavon, C. de Hollanda Cavalcanti, L.T. Tsuha, Monotonic, cyclic and post-cyclic performances of single-helix anchor in residual soil of sandstone, J. Rock Mech. Geotech. Eng. 11 (2019) 824–836, https://doi.org/10.1016/j.jrmge.2018.12.012.
[58] J. Wołoszyn, Global sensitivity analysis of borehole thermal energy storage efficiency for seventeen material, design and operating parameters, Renew. Energy 157 (2020) 545–559, https://doi.org/10.1016/j.renene.2020.05.047.
[59] L. Gao, J. Zhao, Z. Tang, A review on borehole seasonal solar thermal energy storage, Energy Proc. 70 (2015) 209–218, https://doi.org/10.1016/j.egypro.2015.02.117.
[60] H. Mahon, D. O'Connor, D. Friedrich, B. Hughes, A review of thermal energy storage technologies for seasonal loops, Energy 239 (2022), 122207, https://doi.org/10.1016/j.energy.2021.122207.